



Review

Unleashing the potential of adipose organoids: A revolutionary approach to combat obesity-related metabolic diseases

Xingran Liu^{1,2}, Jing Yang^{1,2}, Yuxin Yan^{1,2}, Qingfeng Li^{1,2}, Ru-Lin Huang^{1,2}

1. Department of Plastic and Reconstructive Surgery, Shanghai Ninth People's Hospital, Shanghai Jiao Tong University School of Medicine, Shanghai, China.
2. Shanghai Institute for Plastic and Reconstructive Surgery, Shanghai, China.

✉ Corresponding author: Qingfeng Li, Ph.D., M.D.; (dr.liqingfeng@shsmu.edu.cn); Department of Plastic and Reconstructive Surgery, Shanghai Ninth People's Hospital, Shanghai Jiao Tong University School of Medicine, 639 Zhizaoju Road, 200011 Shanghai, China. Ru-Lin Huang, Ph.D., M.D.; (dr.liqingfeng@shsmu.edu.cn); Department of Plastic and Reconstructive Surgery, Shanghai Ninth People's Hospital, Shanghai Jiao Tong University School of Medicine, 639 Zhizaoju Road, 200011 Shanghai, China.

© The author(s). This is an open access article distributed under the terms of the Creative Commons Attribution License (<https://creativecommons.org/licenses/by/4.0/>). See <http://ivyspring.com/terms> for full terms and conditions.

Received: 2024.01.05; Accepted: 2024.02.15; Published: 2024.02.25

Abstract

Obesity-related metabolic diseases, including obesity, diabetes, hyperlipidemia, and non-alcoholic fatty liver diseases pose a significant threat to health. However, comprehensive pathogenesis exploration and effective therapy development are impeded by the limited availability of human models. Notably, advances in organoid technology enable the generation of adipose organoids that recapitulate structures and functions of native human adipose tissues to investigate mechanisms and develop corresponding treatments for obesity-related metabolic diseases. Here, we review the general principles, sources, and three-dimensional techniques for engineering adipose organoids, along with strategies to promote maturation. We also outline the application of white adipose organoids, primarily for disease modeling and drug screening, and highlight the therapeutic potential of thermogenic beige and brown adipose organoids in promoting weight loss and glucose and lipid metabolic homeostasis. We also discuss the challenges and prospects in the establishment and bench-to-bedside of adipose organoids, as well as their potential applications.

Keywords: Adipose organoid; Obesity; Type 2 diabetes mellitus; Metabolic disease; Brown adipose tissue

1. Introduction

Obesity is a chronic metabolic disease characterized by excessive accumulation of adipose tissue which usually results in a low-grade, chronic, systematic inflammation state [1]. Its worldwide prevalence has nearly tripled since 1975 [2] and affects more than 1 billion people worldwide in 2022 [3]. Moreover, over 4 million people died each year as a result of being overweight or obese [4]. According to the World Health Organization, obesity is defined as a body mass index over 30 kgm², which is calculated by taking a person's weight, in kilograms, divided by their height, in meters squared [5]. Obesity significantly increases the risk of dyslipidemia and insulin-resistance [1], which contribute to the development of type 2 diabetes mellitus (T2DM),

non-alcoholic fatty liver disease (NAFLD), and cardiovascular diseases [6,7]. These metabolic diseases are called obesity-related metabolic diseases (OMDs) [8,9]. Mechanistically, high-fat and high-glucose diets cause energy intake to exceed energy expenditure, thereby contributing to OMD development [10,11]. The pathogenesis of OMDs is not fully understood and current management includes lifestyle intervention challenging to keep [12], as well as medications and surgical interventions with undesired adverse effects [12,13]. However, the lack of authentic and unlimited human models hampers further exploration of pathogenesis and the development of rational therapies with high efficacy and safety.

Organoids are three-dimensional (3D) tissue aggregates derived from stem cells, progenitor cells, and/or differentiated cells that self-organize through cell-cell and cell-extracellular matrix (ECM) interaction to recapitulate structures and functions of native tissue *in vitro* [7,14]. They are miniaturized and simplified model systems of organs that have gained enormous interest for disease modeling, drug screening, and regenerative medicine [15–17]. For OMDs, white adipose organoid (WAO) holds promise in disease modeling to decipher pathogenesis and drug screening for novel drug development. Besides, transplantation of brown adipose organoid (BrAO) and beige adipose organoid (BeAO) exhibits long-term therapeutic potential for OMDs by eliciting weight loss and improving glucose and lipid metabolism. Notably, lifestyle interventions are highly accessible and cost-free options for OMD treatment; however, they necessitate significant personal initiative and a high level of self-discipline. Pharmacologic treatments offer hope to a broader range of OMD patients but require tolerance for the medications' high costs and potential gastrointestinal and psychiatric side effects, as well as ongoing adherence to prevent weight regain [12,18]. Surgery is also a boon for individuals lacking initiative, with bariatric surgery currently demonstrating favorable outcomes in obesity management; nevertheless, it is invasive and associated with complications such as cholelithiasis. Unfortunately, there are no surgical options available for OMDs like T2DM and NAFLD [12]. Transplantation of BrAO and BeAO, like surgery, has the advantage of independence on personal initiative and long-term compliance compared to lifestyle interventions and pharmacological treatments. Moreover, it presents the benefits of being less invasive and universally effective for OMDs compared to surgery.

In this review, we summarize the general principles, sources, and 3D techniques to fabricate adipose organoids, as well as approaches to promote maturation. We also review their current applications in obesity, T2DM, dyslipidemia, and NAFLD and discuss the challenges and prospects for further clinical applications.

2. Adipose organoid, an emerging tool to combat OMDs

To better establish adipose organoids, it is imperative to understand native adipose tissues first. Adipose tissue is a heterogeneous organ with a complex microenvironment and plays a pivotal role in energy homeostasis regulation. White adipose tissues (WATs) containing lipid-accumulated white adipocytes contribute to energy storage; whereas

brown adipose tissues (BATs) and beige adipose tissues both contain adipocytes with high uncoupling protein 1 (UCP1) expression for energy-burning. Adipose tissues also contain mesenchymal stem cells (MSCs), endothelial cells (ECs), immune cells, and neurons [7,19]. The ECM containing collagens and polysaccharides significantly impacts cell survival, adhesion, migration, differentiation, and metabolism [20]. Moreover, adipose tissues secrete adipokines, such as leptin, adiponectin, and batokines (adipokines from brown and beige fat) [21], which mediate communication with livers, skeletal muscles, and satiety centers. Therefore, adipose tissue is considered an endocrine organ, and several reviews have elaborated on adipokines [19,21–23].

For WAT characterized by unilocular adipocytes [7], it stores and releases energy in the form of fatty acids in response to systematic demands [24]. Therefore, WAOs should contain adipocytes with a large unilocular lipid droplet [7], which can be characterized by scanning electron microscopy [25], H&E staining [25,26], AdipoRed [28], BODIPY [25,29], and Oil Red O staining [30], as well as perilipin immunostaining [31]. WAOs should also express common adipogenic markers such as ADIPOQ, FABP4, PPARG, and C/EBPB, as well as specific white markers like LEP, RETN, and AGT [24]. In terms of function, WAOs should at least possess the endocrine function in adipokine secretion [27,28]. Besides, triglyceride accumulation and glycerol release corresponding to energy storage and release *in vivo* are also evaluated sometimes [28]. Notably, excessive lipid accumulation in adipose tissues usually results in insulin-resistance, increased lipolysis, and pro-inflammatory cytokine secretion [23,32]. The hypertrophic WATs contribute to the elevation of peripheral glucose and lipid levels, lipotoxicity in various organs, and further to OMD development [23,32]. Therefore, through fatty acid exposure, TNF- α stimuli, or macrophage co-culture, WAOs can be successfully applied to disease modeling and drug screening of obesity, T2DM, and NAFLD.

Brown and beige adipocytes contain multiple small lipid droplets and numerous cristae-dense mitochondria with high UCP1 expression [21]. Developing embryonically, BATs located in specific regions such as the interscapular region are present only in infancy in humans but are maintained in adulthood in mice [24,33]. Beige adipocytes emerge sporadically in WATs postnatally in response to cold exposure or other certain stimuli [24]. The multilocular structure of adipocytes in BrAOs and BeAOs is usually characterized by phase contrast imaging [34,35], scanning and transmission electron

microscopy imaging [35], H&E staining [36], Oil Red O [37], LipidTox Green [35], and BODIPY staining [38], and perilipin immunostaining [39]. Moreover, dense mitochondria with high UCP1 expression are usually characterized by immunostaining [35,36]. They also express thermogenic markers such as UCP1, DIO2, CIDEA, PPARGC1A, and PRDM16 [24]. However, these are insufficient for distinguishing between brown and beige identities; hence, a test on the expression of specific markers is imperative. It was reported that LHX8, ZIC1, EVA1, and PDK4 are exclusive for classical brown adipocytes, while TBX1, CITED, SHOX2, CD137, and TMEM26 are for beige ones [24,35,40].

In terms of function, brown and beige adipose tissues convert energy into heat by burning fatty acids and glucose through uncoupling respiration. Besides, the batokines usually contribute to metabolic hemostasis through inter-organ communication [19]. Therefore, BrAOs and BeAOs show high-level and β -adrenergic responsive glucose and lipid uptake, lipolysis, and glycolysis, and basal, proton-leak, and maximal oxygen consumption rates (OCR) in vitro [34–36]. The glucose uptake and lipid uptake are assessed by measuring the radioactivity of [3 H]-2-deoxyglucose [41] and [14 C] palmitic acid [41], respectively, and lipolysis is quantified by glycerol release. Besides, the Seahorse bioanalyzer is often used to assess energy extracellular acidification rates for anaerobic glycolysis and OCR for aerobic mitochondrial respiration [35]. BrAOs and BeAOs also secrete batokines which improve insulin-resistance [39] and endogenous adipokine secretion [36]. Therefore, the functions of non-shivering thermogenesis and metabolic healthy secretion enable BrAOs and BeAOs to treat OMDs after transplantation [7,21].

In practice, the term 'adipose organoid' has often been used interchangeably with other terms, such as 'adipose spheroid' [42], 'adipocyte aggregate' [43], 'fat organoid' [44], 'adipose tissue' [38,45], and 'adipose microtissue' [36]. Considering the structures and functions they exhibited, we discuss them uniformly in the term 'adipose organoid' in the following section.

3. Strategies to establish adipose organoids

3.1 General principles to establish adipose organoids

All three adipose tissues rely on the involvement of peroxisome proliferator-activated receptor γ (PPAR γ) and CCAAT/enhancer binding protein α (C/EBP α) for adipogenesis, with their fate bifurcation

occurring at an earlier stage. The development of the three adipose tissues is demonstrated in detail in **Figure 1**. In brief, at the embryonic stage, BATs derive from the dermomyotome of FOXC1 $^+$ MYF5 $^+$ PAX3/7 $^+$ paraxial mesoderm driven by EBF2 and PRDM16 [24], whereas WATs originate from ISL1 $^+$ FOXF1 $^+$ splanchnic mesoderm (SplM) driven by BMP4 [23]. This specification of mediolateral fates of mesoderm is controlled by antagonism of the BMP and WNT signaling pathways [46,47]. Beige adipose tissues are induced from WATs under cold exposure or β -adrenergic stimuli at the postnatal stage [24]. The highly inducible brown-like adipocytes will go whitening to dormant white adipocytes if the stimuli are withdrawn while reinstalling into beige adipocytes after re-exposure to stimuli [21,24,33].

Based on the understanding of the development in vivo, various sources have been applied. State-of-the-art sources include PSCs corresponding to the amniote embryo stage in vivo, ADSCs, stromal vascular fragments (SVFs) from WAT (SVF-WATs), and micro-WATs corresponding to the white adipocyte progenitor stage, as well as SVF-BATs corresponding to the brown adipocyte progenitors stage. Therefore, PSC-derived white adipocyte progenitors, ADSCs, SVF-WATs, and micro-WATs exhibit bipotency. WAOs are derived in the common adipogenic differentiation medium with small molecules that activate PPAR γ and C/EBP α ; whereas BeAOs are generated with additional compounds or gene engineering techniques to mimic the external browning stimuli. PSC-derived brown adipocyte progenitors and SVF-BATs are unipotent to brown adipocytes after adipogenic differentiation. The supplementation of browning compounds could further enhance brown differentiation efficiency.

All sources undergo the adipogenic differentiation process with PPAR γ and C/EBP α being activated synergetically [23,48]. The adipogenic differentiation medium basically consists of insulin, dexamethasone, and 3-Isobutyl-1-methylxanthine (IBMX) with other adipogenic compounds supplemented sometimes. In detail, insulin activates AKT/mTOR signaling pathway [23,49], triiodothyronine (T3) activates thyroid hormone receptor [50], and indomethacin inhibits cyclooxygenase [51] to promote PPAR γ activation. Meanwhile, rosiglitazone directly activates PPAR γ [52]. In addition, glucocorticoids such as dexamethasone activate C/EBP δ [23,36,53], cyclooxygenase inhibitors such as indomethacin activate CEB/P β [51], phosphodiesterase inhibitors such as IBMX increase cAMP [54,55], and TGF- β inhibitors such as SB-431542 down-regulate intracellular SMAD3 expression [35,56] to induce C/EBP α activation. Additionally, type B vitamins

such as biotin [29,41,57,58], pantothenate [29,41,57,58], and apo-transferrin [58] and type C vitamins [40,53,57,59,60] are usually supplemented.

For browning, PRDM16 plays a pivotal role in driving the thermogenic program [24] with the assistance of EBF2 in the early stage [39] and PGC-1 α to co-activate several transcriptional factors [61]. Besides, PPAR γ also contributes to the thermogenic program by increasing the half-time of PRDM16 [24,62]. T3 [29,41,63] and rosiglitazone [36,63–66] mentioned above are common browning compounds. Particularly, T3 promotes browning by supporting BAP proliferation [67] and stimulating PGC-1 α [68] and UCP1 [39,63,69–71]. TGF- β inhibitors [36] also promote browning by activating EBF2 [39]. Besides, BMP7 activates PRDM16 [37] and promotes mitochondrial biogenesis by activating the p38 MAPK signaling pathway [40,64]. Additionally, ROCK inhibitors such as Y-27632 [64] and transferrin [65,72] are also sometimes included in the browning medium. β -adrenergic agonists such as mirabegron and CL316,243 and cAMP activators such as forskolin,

which directly mimic external β -adrenergic stimulation in vivo, also contribute to the generation of BrAOs and BeAOs in vitro [34,73].

3.2 Sources for adipose organoids

3.2.1 PSCs

Previously, researchers differentiated PSCs into embryonic bodies (EBs) in suspension and derived a mixture of MSCs after transferring them to adherent plates. Retinoic acid pretreatment combined with CD73 selection [53,74] or PPAR γ transduction [48] generated HOXC8/9⁺ HOXA5⁺ BMP4⁺ white adipocyte progenitors. Meanwhile, CD73 selection without retinoic acid pretreatment [53,74] or PRDM16 [75], PPAR γ 2-CEB/P β [48], or PPAR γ 2-CEB/P β -PRDM16 [48] transduction enabled PAX3⁺ CIDEA⁺ CD137⁺ brown adipocyte progenitors. The derived white and brown adipocyte progenitors differentiated into white and brown adipocytes, respectively.

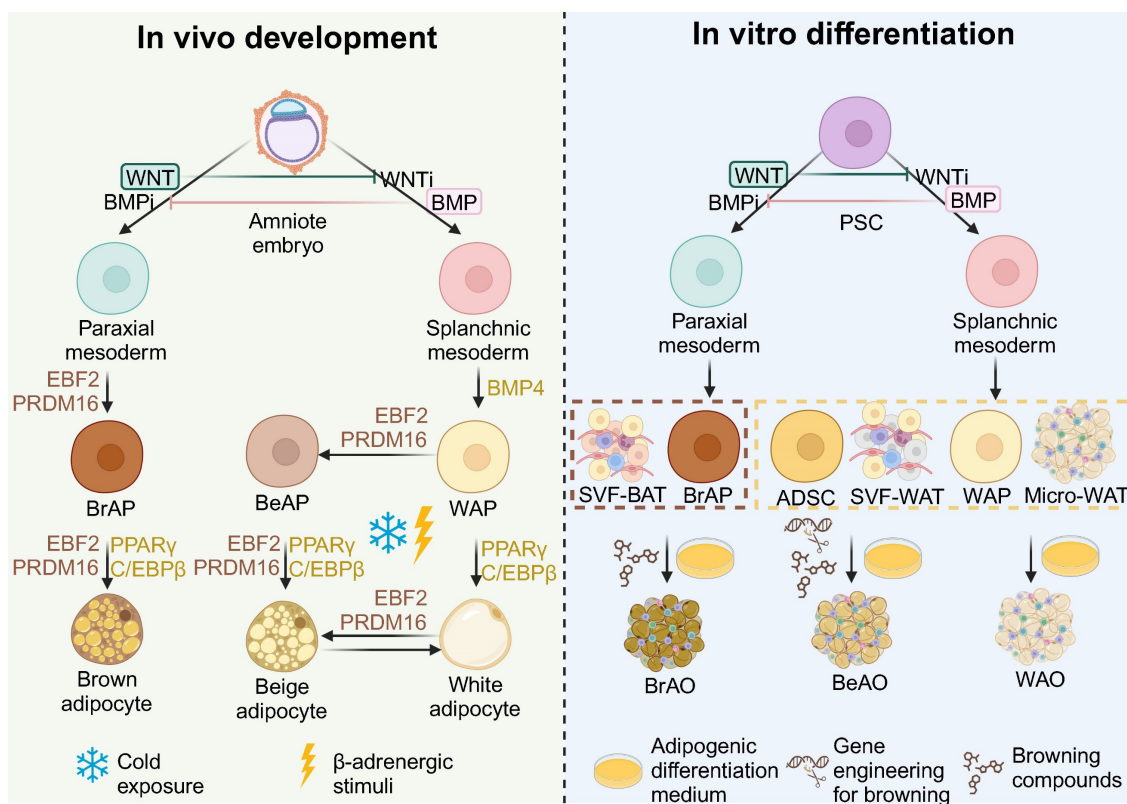


Figure 1. General principles to generate adipose organoids in vitro based on the in vivo development of adipose tissues. Based on the understanding of the development in vivo, by modulating WNT and BMP signaling pathways, brown and white adipocyte progenitors going through paraxial and splanchnic mesoderm, respectively, are induced from pluripotency stem cells (PSCs). Brown adipocyte progenitors from PSCs and stromal vascular fragments from brown adipose tissues correspond to the brown adipocyte progenitor stage in vivo which are fate-determined to brown adipocytes. Therefore, brown adipose organoids can be derived in the basic adipogenic differentiation medium through activation of PPAR γ and C/EBP α , key factors of adipogenesis; while supplementation of browning compounds that mimic the EBF2 and PRDM16 activation in vivo can further enhance the differentiation efficiency. White adipocyte progenitors from PSCs, adipose-derived stem cells, stromal vascular fragments from white adipose tissues, and micro white adipose tissues correspond to the white adipocyte progenitor stage in vivo which is bipotent. Therefore, white adipose organoids can be derived in the basic adipogenic differentiation medium. With additional genetic engineering techniques to introduce thermogenic genes and/or supplementation of browning compounds to mimic the cold exposure or β -adrenergic stimuli that activate EBF2 and PRDM16 in vivo, beige adipose organoids can be successfully induced from these bipotent sources. ADSC: adipose-derived stem cell; BeAO: beige adipose organoid; BeAP: beige adipocyte progenitors; BrAO: brown adipose organoid; BrAP: brown adipocyte progenitor; Micro-WAT: micro white adipose tissue; PSC: pluripotent stem cell; SVF-BAT: stromal vascular fragment from brown adipose tissue; SVF-WAT: stromal vascular fragment from white adipose tissue; WAO: white adipose organoid; WAP: white adipocyte progenitor.

However, these strategies did not undergo defined mesoderm stages, thus causing the identity of derived brown adipocytes to be questioned [35]. Based on current knowledge about adipose tissue development, several studies have designed stepwise methods to derive beige and brown adipocytes [57]. BMP4 plays an essential role in the commitment of SplM from PSC to derive beige adipocytes [39,60]. Guénantín et al. induced hiPSCs to PDGFRA⁺ LY6E⁺ CD29⁺ beige adipocyte progenitors in a hematopoietic medium containing BMP4 and Activin A⁶⁵. Besides, Su et al. induced hiPSCs to SplM by activating the BMP, WNT, and VEGF signaling pathways [39]. They overcame the adipogenic differentiation limitation of FOXF1⁺ SplM-derived MSCs by inhibiting TGF- β and activating IL-4. The derived beige preadipocytes differentiated into beige adipocytes in the adipogenic differentiation medium supplemented with browning compounds [39]. These SplM-derived beige adipocytes exhibited high-level and β -adrenergic responsive OCR [39]. They also secreted anti-T2DM adipokines to improve the glucose metabolism of white adipocytes from T2DM patients [39,60].

Activation of WNT and FGF signaling pathways, along with BMP inhibition, are crucial for the commitment of paraxial mesoderm from PSCs to obtain brown adipocytes [35,57]. Zhang et al. induced hiPSCs to PAX3⁺ MYF5⁺ FOXC1⁺ paraxial mesoderm by activating WNT and FGF while inhibiting the BMP signaling pathway. Paraxial mesoderm eventually differentiated into mature brown adipocytes with high-level and responsive glycolysis, lipolysis, and OCR. Besides, they increased thermogenesis and energy expenditure, and improved glucose homeostasis of hyperglycemia mice after transplantation [35]. Similarly, Carobbio et al. induced MYF5⁺ PDGFR α ⁺ paraxial mesoderm from hESCs by activating WNT, FGF, and retinoic acid signaling pathways and then to brown adipocyte precursors with BMP inhibitors such as LDN-193189 supplemented. They eventually derived KCNK3⁺ MTUS1⁺ ITGA10⁺ multilocular brown adipocytes after adipogenic differentiation [57].

3.2.2 Cells derived from adipose tissues

Cells derived from adipose tissues capable of the generation of adipose organoids include ADSCs, SVF-WATs, and SVF-BATs. ADSCs are commonly used for WAOs while browning molecules [64,65,72] are necessary for white-to-beige transition [27,31,64,65,72,76]. Singh et al. realized the beige differentiation efficiency of ADSCs to over 90% by supplementing T3, rosiglitazone, BMP-7, and Y-27632 in adipogenic differentiation medium [64]. Beige adipocytes exhibited higher levels of cAMP-sensitive

uncoupled respiration, glycolysis, and lipolysis compared with white adipocytes [64]. SVFs contain heterogeneous subpopulations of cells, including endogenous ECs and immune cells [7], thus showing advantages in vascularization and modeling inflammation. Immortalization of SVFs clearly described in articles [34,63] is necessary for application. The fate of SVFs is predetermined; therefore, basal adipogenic differentiation medium supplemented with T3 is sufficient for the differentiation of SVF-WATs and SVF-BATs [29,41,63]. Browning molecules can enhance the differentiation efficiency of SVF-BATs [36] but have limited impact on promoting the white-to-beige transition of SVF-WATs [41]. With T3 and rosiglitazone supplemented to augment browning efficiency, brown adipocytes differentiated from SVF-BATs exhibited higher levels of maximum and uncoupled OCRs in both basal and cAMP-stimulated states, glucose uptake in basal and insulin-stimulated states, as well as fatty acid uptake and oxidation [41,63]. Wang et al. successfully realized the white-to-beige transition of SVF-WATs by activating endogenous UCP1 using CRISPR-Cas9. Such brown-like adipocytes exhibited higher levels of glucose uptake, glucose-dependent and fatty acid-dependent uncoupled OCRs, and thermogenic capacity compared with white adipocytes [77].

3.2.3 Adipose tissues

Micro adipose tissues maintain complex cellular and ECM components for a fidelity microenvironment in adipose organoids [28]. Micro-WATs are usually obtained by cutting subcutaneous adipose tissues (SATs) into small pieces (0.5-5 mm) [34,78], mincing through 19-gauge needles, or liquefying in a blender through continuous short pulses. Through embedding fragments of the rat superficial fascia (1-3 mm³) in fibrin hydrogels, seeding liquified human lipoaspirates into silk scaffolds, or sandwiching human primary WAT fragments (0.5-1 mm) between SVF-derived adipose sheets, WATs were reconstructed to maintain viable and functional for longer time (over 3 months) [28,79] than primary explants. These WAOs exhibited unilocular structure and functions in lipogenesis [28,44], lipolysis [28,44,79], and adipokine secretion [28,44,79]. To generate BeAOs from micro-WATs, β -adrenergic agonists, cAMP activators, and angiogenic compounds are usually supplemented. Blumenfeld et al. directly converted both SAT and visceral adipose tissue (VAT) fragments into 'brown' adipose organoids in adipogenic differentiation medium supplemented with T3, rosiglitazone, CL316,243, and VEGF for 3 weeks. The organoids

contained multilocular adipocytes with high UCP1 expression and mitochondrial metabolic activity. They maintained the thermogenic phenotype for at least 8 weeks after transplantation [73]. However, considering the SplM origin, such 'brown' adipose organoids might theoretically be BeAOs which requires further validation.

3.3 3D techniques for adipose organoids

In addition, the role of the 3D microenvironment for adipose organoids is also unneglected. Compared with traditional 2D culture, 3D shows the following advantages: 1) 3D maintains depot-specific characteristics [80]; 2) 3D increases cell-cell adhesion and crosstalk [80]; 3) 3D links the organotypic microenvironment to improve adipogenesis [26,81–84]; 4) 3D is more responsive to insulin and pro-inflammatory stimuli and sensitive to metabolic and environmental stress [26,85,86]; 5) 3D promotes stemness and long-term survival [82,85]; 6) 3D is feasible to manipulate biochemical, mechanical, topographic, and cellular microenvironment [29,85]; 7) 3D secretes higher levels of adipokines such as

adiponectin [26]. Current 3D techniques for adipose organoids are summarized in **Figure 2**.

3.3.1 Scaffold-free techniques

For scaffold-free techniques, cells are exposed to a non-adherent environment to attach to each other, synthesize and remodel their own ECM, and finally form a 3D agglomerate through cell-cell and cell-matrix interaction. For the ultra-low attachment technique, ADSCs [87,88], SVFs [81,89–91], or preadipocytes [86] were seeded in ultra-low attachment microwells in static culture [81,86,87, 89,90,92], or dynamic culture involving stirring [91] or shaking [88]. It also enabled the establishment of disease models from ADSCs of lipedema patients [88] and perinephric adipose tissue SVFs of kidney tumor patients [89]. Notably, Turner et al. designed elastin-like polypeptide (ELP)-polyethyleneimine (PEI)-coated 24-well plates to establish 45 μm adipose spheroids by seeding 50,000 3T3-L1 preadipocytes [86] or ADSCs [92] per well. The ELP promotes spheroid formation, and PEI promotes spheroid attachment to the surface. Such 3D spheroids

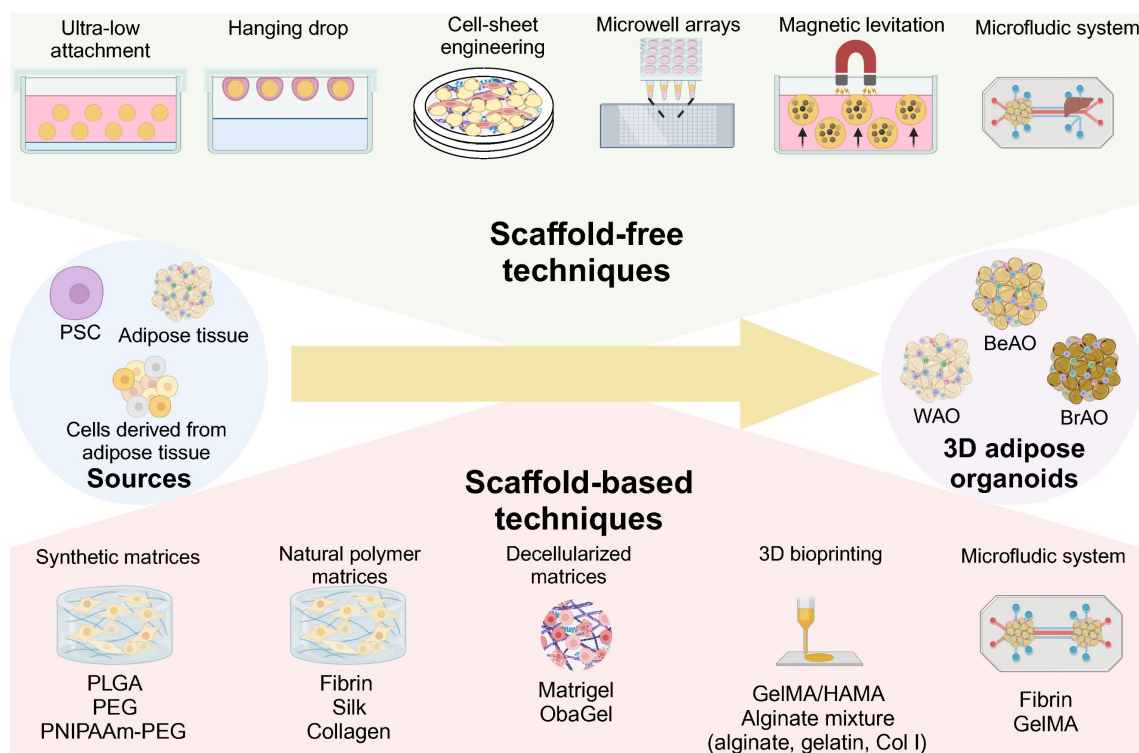


Figure 2. Scaffold-free and scaffold-based strategies to establish 3D adipose organoids. Through three-dimensional (3D) techniques including scaffold-free and scaffold-based techniques, 3D adipose organoids can be fabricated from various sources. The ultra-low attachment technique is the most widely used scaffold-free technique due to its automation, simplicity, and high throughput. The hanging drop technique enables precise size control, but is challenging to replenish the low-volume culture medium. Cell-sheet engineering enables the generation of adipose organoids through superposition. Microwell arrays perform well in precisely controlling the diameters of adipose organoids by limiting seeded cell numbers. The magnetic levitation technique also enables the establishment of adipose organoids composed of more than one cellular component through positive or negative magnetophoresis. The microfluidic device provides a chance to recapitulate the communication between adipose tissues and other organs. Scaffold-based techniques include synthetic, natural polymer, and decellularized matrices that can be used alone or in combination with 3D bioprinting and microfluidic systems. Scaffolds promote cell attachment and migration and inhibit excessive cell aggregation. They also promote sprouting, adipogenesis, maintenance of depot-specific and subject-specific characteristics, and long-term preservation of viability and function of adipose organoids. BeAO: beige adipose organoid; BrAO: brown adipose organoid; Col I: type I collagen; dECM: decellularized extracellular matrix; GelMA: methacrylate gelatin; HAMA: hyaluronic acid; PEG: poly(ethylene-glycol); PLGA: poly(lactic-co-glycolic acid); PNIPAAm: poly(N-isopropylacrylamide); PSC: pluripotent stem cells; WAO: white adipose organoid; 3D: three dimensional.

outperformed the 2D monolayer adipocytes in responsiveness to fatty acid exposure and TNF- α stimuli for obesity modeling [86,92]. Through the hanging drop method, preadipocytes [93], SVFs [26], ADSCs [58], or microvascular fragments (MVs) [94] self-assembled due to gravity. The cell suspension of 20-28 μ l per droplet was placed on the inside lid of the plate and inverted for 2-5 days to form spheroids due to gravity [26,58,93,94]. Quan et al. generated well-vascularized adipose organoids (300-400 μ m in diameter) exhibiting responsive lipolysis and adipokine secretion [94]. Adipose organoids (150 μ m in thickness) were also reconstructed via the superposition of three adipose sheets derived from ADSCs in adipogenic differentiation medium supplemented with Vitamin C [27,79,95-97]. Adipose organoids remained viable for at least 11 weeks and secreted higher levels of leptin, plasminogen activator inhibitor-1, and angiopoietin-1 than primary fat explants [97].

Considering the high demand for glucose, oxygen, and nutrients of thermogenic adipocytes, precise control of the diameter of BrAOs or BeAOs is crucial [36]. Microwell arrays perform well in the production of size-controlled organoids. Oka et al. generated adipose spheroids (100-120 μ m in diameter) by seeding hPSCs on the Elplasia® 3D discovery tool with 90 microwells per well to restrict cell numbers within a range of 2,000-2,500 cells for each spheroid formation [98]. They derived BrAOs containing multilocular adipocytes with dense mitochondria in the aforementioned hematopoietic medium [98]. These BrAOs with optimal diameters secreted batokines which promote insulin secretion of β cells and maintained thermogenic capacity after transplantation [98]. For the magnetic levitation technique, mice SVFs [99] or preadipocytes [100] were mixed with nanoshuttles to be magnetically levitated in positive magnetophoresis for aggregation [99,100]. The derived WAOs recapitulated the molecular signaling pathway of WAT organogenesis [99,100] and complex vascularized structures through co-culture with ECs [100]. However, unremovable nanoshuttles may induce DNA cytotoxicity once internalized [101,102]. Sarigil et al. first demonstrated the utilization of the negative magnetophoresis for WAO establishment from adipocytes and even multilayered ones by co-culturing with bone marrow-derived mesenchymal stem cells. This label-free method holds potential for clinical regenerative medicine if further function validation can be conducted [103]. Microfluidic devices supported complete on-chip differentiation of human preadipocytes to form WAOs responsive to proinflammatory, obese, and diabetic conditions. This

organ-on-chip technology successfully recapitulated communication between adipose tissues and livers [104].

3.3.2 Scaffold-based techniques

Besides, other strategies utilized scaffolds containing ECM or ECM-like components for the 3D adipose organoid formation via cell-matrix interaction. Common scaffolds including synthetic, natural polymer, and decellularized matrices promote cell attachment and migration while inhibiting excessive cell aggregation. The physicochemical environment of matrices also affects white and brown adipogenesis, maintenance of depot-specific characteristics, and metabolic functions [29,36,105,106]. However, the safety and ethical concerns of synthetic and animal-derived hydrogels hinder their further clinical application. Therefore, thermoreversible poly(N-isopropylacrylamide)-poly(ethylene-glycol) (PNIPAAm-PEG) hydrogels and human-derived decellularized ECMs (dECMs) have been designed for better bench-to-bedside translation [36,107].

Synthetic matrices commonly include porous poly(lactic-co-glycolic acid) (PLGA) hydrogels and PEG-based hydrogels. The porous PLGA hydrogels promoted the generation of size-controlled WAOs (220 μ m in diameter) with angiogenic adipokine secretion [76]. PEG-based hydrogels are easy to modify, like with RGD-containing peptides to further promote initial cell attachment and adipogenic differentiation [106]. Besides, Wang et al. designed thermoreversible PNIPAAm-PEG hydrogels to form size-controlled BrAOs with high yield (1×10^7 cells/ml hydrogel). PNIPAAm-PEG hydrogels enabled ideal short-term preservation at room temperature and long-term cryopreservation without sacrificing viability and could be easily removed before transplantation [36].

For natural polymer matrices, fibrin hydrogels promoted superficial fascia fragments [44], ADSCs [25,31,108], and MVs [38] to form WAOs containing unilocular adipocytes with lipolysis and adipokine secretion functions [25,31,44,108]. Thin fibrin-based cellulose scaffolds further supported the assembly of WAOs sensitive to fatty acid exposure to model obesity [25]. By seeding human liquified lipoaspirates in silk scaffolds, fragile WATs can be endocrinologically functional for the long term. Considering the availability of a small volume of lipoaspirates, this method holds potential for studying patient-specific drug response and pathogenesis [28,78]. Meanwhile, fibrin promoted the maintenance of subject-specific differences between lean and T2DM patients [38], while collagen

supported the preservation of depot-specific characteristics [105].

For decellularized matrices, Matrigels facilitate the sprouting of SVFs and micro-WATs to derive beige adipocyte progenitors in angiogenic endothelial growth medium (EGM) [34,91]. To address the ethical concerns, human blood-derived ObaGels were designed to generate human SVF-derived WAOs capable of lipolysis, glucose uptake, and leptin secretion [107]. In particular, the proteomic profile and physical microenvironment of dECMs show differences between obese and lean donors, with a pro-inflammatory microenvironment in the former [109]. Therefore, subject-specific dECMs should be further applied to patient-specific adipose organoid generation [110].

Besides, methacrylate gelatin and hyaluronic acid (GelMA/HAMA) hydrogels and alginate hydrogel mixture are commonly employed as bioinks for 3D bioprinting. GelMA/HAMA hydrogels enabled the study of optimal mechanical conditions for different adipocyte adipogenesis. It was found that soft solid hydrogels efficiently promoted white adipogenesis, whereas stiff porous hydrogels promoted brown adipogenesis [29]. 3D-printed BrAOs in the alginate hydrogel mixture exhibited high UCP1 expression [111], while WAOs mimicked insulin-resistance through macrophage co-culture for disease modeling and drug screening of T2DM [83,84,112]. Paek et al. designed a hybrid microfluidic platform containing perfusable microchannels in a fibrin hydrogel to establish well-vascularized WAOs with ideal leptin secretion [31]. Besides, by embedding ADSCs from infrapatellar fat pads of osteoarthritis patients, O'Donnell et al. first cultured patient-specific WAOs with robust viability and adipogenesis in both static and dynamic conditions in a perfusion bioreactor to study the role of infrapatellar fat pads in osteoarthritis progression [113].

3.4 Strategies to improve adipose organoid maturation

Vascularization and the incorporation of immune cells can improve the maturity of adipose organoids. Vascularization promotes adipogenesis and browning, as well as facilitates integration with host vessels for long-term maintenance of implants [36,80]. In detail, adipocytes near vessels exhibit superior lipid accumulation [114]. Meanwhile, angiogenic cocktails promote beige preadipocyte proliferation and enhance brown differentiation efficiency [29,34,38,40,53]. Therefore, more studies have focused on the vascularization of BeAOs and BrAOs. Through co-culture with macrophages, WAOs mimicked the mild and chronic inflammation state

and the progression of insulin-resistance in T2DM. However, both the incorporation of macrophages into BeAOs and BrAOs and other immune cells into adipose organoids to better recapitulate cell crosstalk are nascent study areas that need to be further investigated [83,84,112,115].

3.4.1 Promoting vascularization

The incorporation of exogenous or endogenous ECs promoted the vascularization of adipose organoids. Through pre-exposing human co-cultured ADSCs and ECs or BAT-SVFs to angiogenic EGM before adipogenic induction, adipose organoids were well vascularized [31,36] and innervated after transplantation and showed therapeutic effects on obese and T2DM mice [36]. For MVFs, pre-exposure to growth medium just promoted vascularization [38]. Besides, adipose sheets co-cultured with ECs were vascularized with unimpaired leptin secretion function through post-exposure to angiogenic EGM at the later stage of adipogenic differentiation [96,97]. Moreover, the all-in-one medium by mixing adipogenic differentiation medium with EGM in a 1:1 ratio also promoted the generation of vascularized adipose organoids responsive to hyperinsulinemia from co-cultured ADSCs and ECs [116].

Notably, vascularization exerts an active effect on thermogenic programs by activating PRDM16 and UCP1 via the p38 MAPK signaling pathway [40,59]. Pre-exposure to EGM promoted beige preadipocyte proliferation around sprouting vessels from micro-WATs embedded in Matrigels [34]. Moreover, hematopoietic cocktails (IGF-IL, VEGFA, KITLG, FLT3LG, and IL-6) supplemented with BMP4 and then BMP7 directly induced hiPSCs into brown adipocytes with high-level and responsive UCP1 expression and OCR [40]. The brown adipocytes promoted lipid and glucose metabolic hemostasis after transplantation and secreted hematopoietic adipokines potential for myelosuppression treatment [40]. Size-controlled BrAOs, further established in microwell arrays using the same hematopoietic recipes, secreted batokines capable of augmenting the insulin secretion of β cells (**Figures 3A-C**) [98]. Notably, VEGFA [73] and retinoic acid [59] also promoted the browning of adipose organoids through increasing vascularity by activating VEGFA/VEGFR2 signaling [59].

3.4.2 Incorporating immune cells

WAOs incorporated with macrophages better mimicked insulin-resistance compared with monocultured ones validated by proteomic analysis [112]. In addition to co-culturing mice 3T3-L1-derived adipose organoids with mice macrophages, by

loading mice macrophages and human ADSC-derived WAOs in designed separate wells with interaction preserved, errors resulting from interspecies variation can be minimized for further preclinical research (**Figure 3D**) [83,84]. Furthermore, direct induction of SVFs shows the potential to solve the species issue by preserving resident immune cells in adipose organoids. After adipogenic differentiation without any additional immune cell growth factors supplemented, CD45⁺CD31⁻ immune cells in mice SVFs were maintained, which can be attributed partly to the abundant macrophage colony-stimulating factors secreted from undifferentiated adipose organoids. Among the immune cell populations, 60–70% were CD11b⁺F4/80⁺ macrophages, while approximately 10% were FcεR1⁺ckit⁺ mast cells. Therefore, SVF-derived WAOs serve as an ideal

platform for modeling inflammatory states and investigating cell crosstalk between immune cells and adipocytes (**Figure 3E**).

Human SVFs should be further applied to the establishment of human adipose organoids with immune cells retained. Currently, only monocytes and macrophages have been incorporated in WAOs. However, *in vivo*, eosinophils and Tregs secrete factors that induce M2 polarization for adipose tissue homeostasis, while neutrophils, CD8⁺ cells, NK cells, Th1 cells, and B2 cells induce M1 polarization in hypertrophic adipose tissues [23,117]. Eosinophils and M2 also enhance the activity of brown and beige adipocytes [24,118]. Therefore, subsequent studies should attempt to incorporate these immune cells into adipose organoids.

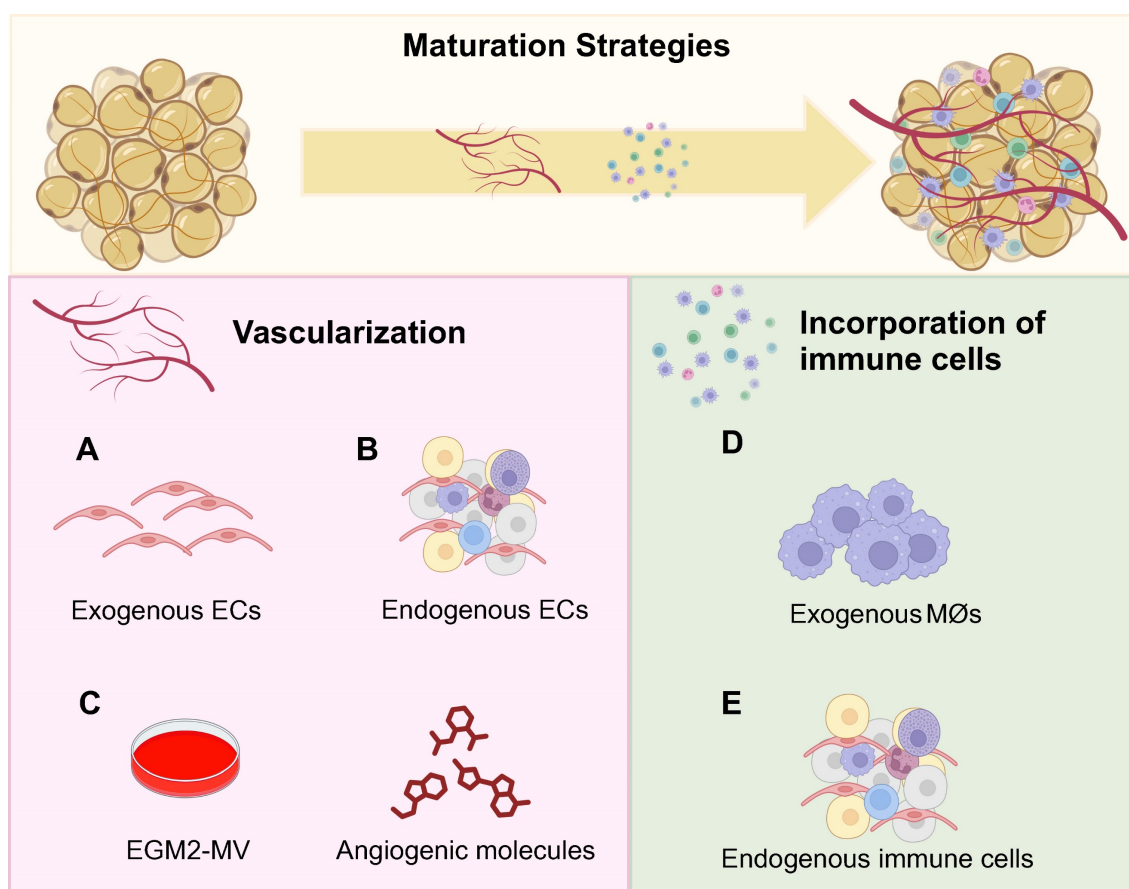


Figure 3. Promoting vascularization and incorporating immune cells to facilitate maturation of adipose organoids. Considering the native adipose tissue niche, both vascularization and immune cell incorporation are crucial for the maturation of adipose organoids. Regarding research intensity, vascularization has been predominantly investigated in brown adipose organoids and beige adipose organoids to promote browning. Although incorporating immune cells is essential for all types of adipose organoids, currently only mice macrophages were successfully incorporated into white adipose organoids for disease modeling and drug screening. No studies have generated brown or beige adipose organoids with macrophages incorporated yet. By incorporating exogenous human microvascular endothelial cells and human umbilical vein endothelial cells (a), or using stromal vascular fragments, microvascular fragments, and adipose tissue explants with endogenous endothelial cells (b), well-vascularized adipose organoids can be successfully generated. (c) The supplementation of angiogenic compounds such as VEGF, IL-6, KITLG, and FLT3LG, along with endothelial growth medium further promotes vascularization, beige preadipocyte proliferation, and *ex vivo* browning. (d) By co-culturing mice macrophages, RAW264.7, with mice 3T3-L1 preadipocytes or human adipose-derived stem cells in alginate hydrogel mixture by three-dimensional bioprinting, inflamed white adipose organoids with insulin-resistance were successfully generated. (e) By directly inducing the adipogenic differentiation of stromal vascular fragments, adipose organoids with resident CD45⁺ CD31⁻ immune cells preserved such as macrophages and mast cells were generated. BeAO: beige adipose organoid; BrAO: brown adipose organoid; EC: endothelial cell; EGM2-MV: endothelial cell growth medium 2-microvascular; Mφ: macrophage; WAO: white adipose organoid.

4. Applications of adipose organoids in obesity-related metabolic diseases

4.1 Obesity

As previously mentioned, obesity caused by excessive energy uptake is characterized by adipose tissue inflammation. Current treatment strategies encompass lifestyle intervention which is challenging to keep, complex medications associated with adverse gastrointestinal or neuropsychiatric effects, and bariatric surgery with complications such as cholelithiasis [12]. Therefore, through lipid exposure, pro-inflammatory stimuli, or co-culture with macrophages, WAOs are capable of disease modeling and drug screening of obesity to identify novel therapies with high safety and efficacy. Moreover, BrAO and BeAO transplantation can realize long-term and stable weight loss primarily by increasing energy expenditure.

Obesity was successfully modeled by exposing WAOs to fatty acids. Extra saturated palmitic or stearic acids, unsaturated oleic acids, or a natural lipid mixture induced an increase in droplet sizes and basal lipolysis [25,86,119,120], correlated with an increase in circulatory levels of fatty acid and glycerol in vivo [86,120]. Fatty acid exposure also induced insulin-resistance and pro-inflammatory cytokine secretion [25,120]. Moreover, the ratio of adiponectin to leptin secretion was reduced, which indicates adipose tissue dysfunction and the development of a pro-inflammatory obesogenic state [120]. Pieters et al. embedded ADSCs in fibrin/Geltrex™ hydrogels and infiltrated them into thin cellulose scaffolds to efficiently assemble WAOs. Exposure to fatty acids effectively enabled obesity modeling with increased lipid droplet sizes and induced insulin-resistance. Specifically, palmitic acids instead of oleic acids increased basal lipolysis and secretion of pro-inflammatory cytokines which alter macrophage gene expression [25].

Another approach for obesity modeling is to expose WAOs to TNF- α or co-culture them with macrophages under lipopolysaccharide (LPS) stimuli. TNF- α and IL-1 β treatment resulted in an increase in pro-inflammatory cytokine secretion and a detrimental effect on the microvascular network in vascularized adipose sheets [95]. Abbott et al. established WAOs by seeding small volumes of liquified lipoaspirates from different individuals into silk scaffolds, enabling assessment of individual responses to TNF- α and serving as a proof-of-concept for future patient-specific preclinical studies [28]. Surprisingly, there were no significant differences in glucose uptake and lipid accumulation under TNF- α

stimuli among WAOs derived from subjects with different body mass indexes [78].

The incorporation of immune cells under LPS stimuli also successfully induced inflammation of WAOs. Harms et al. designed membrane mature adipocyte aggregate cultures to maintain depot-specific characteristics of mature adipocytes for long-term culture and placed macrophages on top of the membrane under LPS treatment. A higher increase in IL-6 and IL-8 secretion of adipocytes and TNF- α and IL-6 secretion of macrophages was induced than in mono-culture [43]. For SVF-derived WAOs with resident immune cells, LPS stimuli also significantly increased the secretion of IL-6 and the obesity-induced chemokine C-C Motif Chemokine Ligand 2 as well as induced a decrease in diacylglycerol and an increase in cholesterol (**Figure 4A**) [119]. Besides, WAOs can further mimic long-term chronic inflammation of adipose tissue through FGF2 exposure to induce fibrosis (**Table 1**) [121].

Adipose organoids can also be applied to high-throughput screening of anti-obesity drugs. Choi et al. formed WAOs by co-culturing mice preadipocytes and macrophages in alginate mixture hydrogel beads. This 3D co-culture system served as a successful high-throughput screening platform validated by its sensitive and dose-dependent responses to rosiglitazone and GW9662 compared with 2D co-culture. Using AdipoRed/dsDNA to evaluate the percentage of adipogenesis inhibition as the first hit, seven compounds exhibiting opposite effects in 3D versus 2D were selected among 178 compounds consisting of adenosine monophosphate-activated protein kinase activators, PPAR γ agonists, and PPAR γ antagonists. Then, three compounds exhibiting repetitive anti-adipogenic effects in 3D were selected by investigating IC₅₀ values [122]. Besides, the easily generated WAOs derived from liquefied lipoaspirates show promise in personalized medicine, as evidenced by their patient-specific responses to AICAR [78]. Combined with high-content confocal and epifluorescence analysis to distinguish well-differentiated spheroids from undifferentiated ones, human SVF-derived WAOs also show potential for high-throughput screening of anti-obesity drugs (**Figure 4B** and **Table 2**) [26].

Transplantation of brown [65] and beige adipocytes [64] as well as BrAOs [36,73] reduced body weight [36,64,65,73] and fat mass [36,73], showing significant less weight and fat mass gains compared to the control group with hADSC [65,123] or white fat explants [73] being transplanted or the sham group [36] 2-26 weeks after transplantation. These results were attributed to the significantly enhanced energy

expenditure resulting from the non-shivering thermogenesis of transplanted thermogenic adipocytes. Specifically, a significantly higher value of volume of oxygen, energy expenditure, as well as core and surface temperature compared to the control group

were simultaneously observed post-transplantation [64]. Meanwhile, as mentioned before, obesity is characterized by a state of low-grade and systematic inflammation.

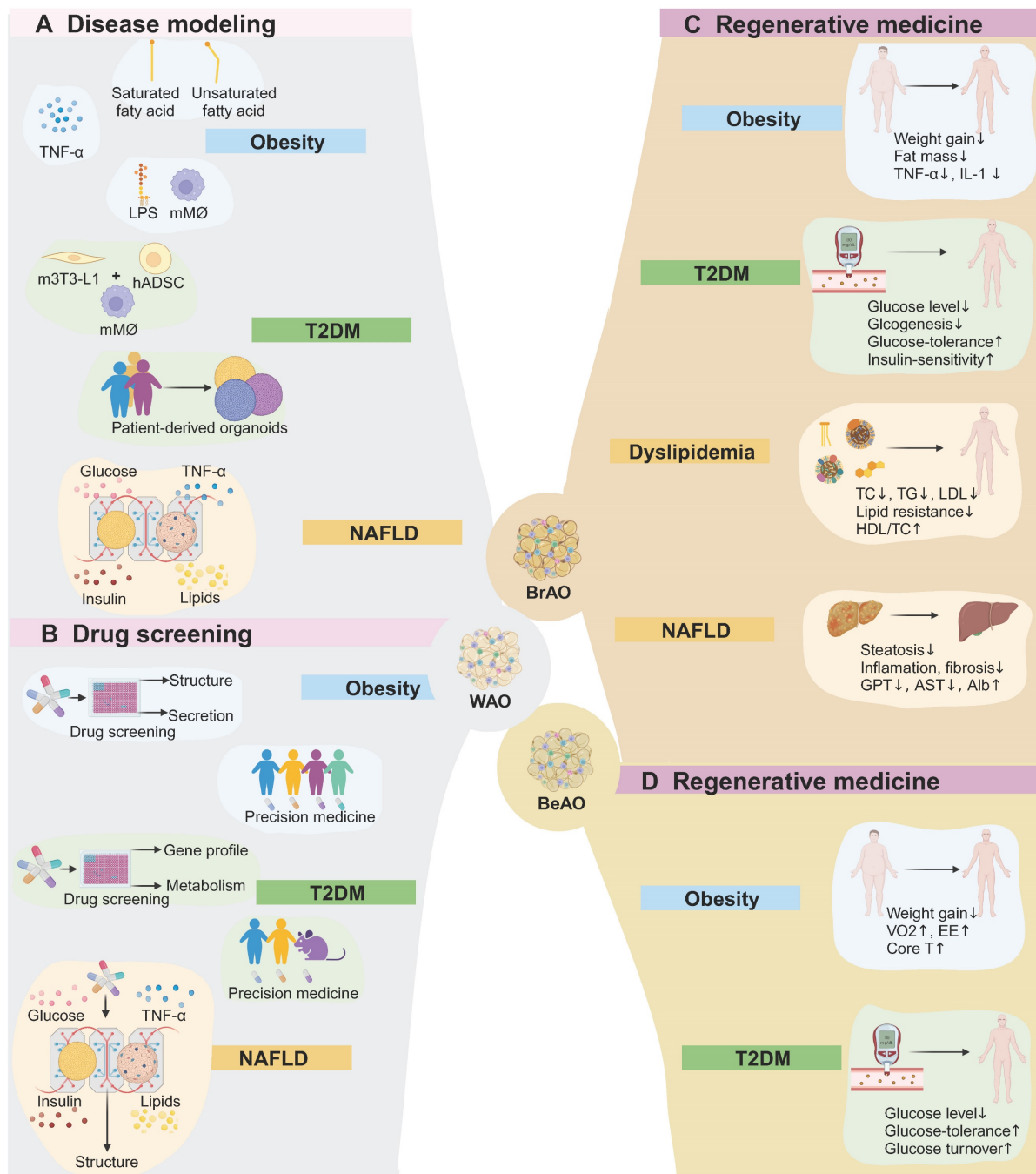


Figure 4. Application of adipose organoids in disease modeling, drug screening, and regenerative medicine. (a) White adipose organoids can model obesity through exposure to fatty acids or TNF- α , or co-culture with immune cells under lipopolysaccharide stimuli. Disease modeling of type 2 diabetes mellitus (T2DM) can be established through co-culture adipose organoids with macrophages, or from patient-derived adipose organoids. Besides, a microfluid system is applied to investigate the role of adipose tissues in the progression of non-alcoholic fatty liver disease (NAFLD) by mimicking healthy, obese, diabetic, and pro-inflammatory plasma conditions. (b) By assessing the effects of compounds on lipid accumulation, adipogenic gene expression, pro-inflammatory cytokine secretion, and metabolism such as glucose uptake, white adipose organoids can be applied to high throughput drug screening and personalized precision medicine in obesity, T2DM, and NAFLD. (c) Brown adipose organoids reduce body weight and fat mass as well as relieve inflammation after transplantation. Transplantation also shows therapeutic potential in T2DM by reducing glucose levels and improving glucose intolerance and insulin-resistance. Besides, it regulates dyslipidemia, relieves inflammation and fibrosis in livers, and improves liver function. (d) Beige adipose organoid transplantation shows potential for treating obesity. Additionally, it also reduces glucose levels and improves glucose tolerance and turnover. Alb: albumin; AST: aspartate transaminase; BeAO: beige adipose organoid; BrAO: brown adipose organoid; Core T: core temperature; EE: energy expenditure; GPT: glutamate pyruvate transaminase; hADSC: human adipose-derived stem cells; HDL/TC: the ration of high-density lipoprotein to total cholesterol; LDL: low-density lipoprotein; LPS: lipopolysaccharide; mM ϕ : mice macrophage; m3T3-L1: mice preadipocytes; NAFLD: non-alcoholic fatty liver disease; TC: total cholesterol; TG: triglyceride; T2DM: type 2 diabetes mellitus; VO $_2$: maximum volume of oxygen; WAO: white adipose organoid.

Table 1. Studies establishing adipose organoids as disease models for obesity-related metabolic diseases

Diseases	Studies	Sources	Methods	Mechanisms	Highlight Results
Obesity	Pieters et al. (2022)[25]	hADSCs	Embedde in fibrin/Geltrex™ hydrogels, and infiltrated into a thin cellulose scaffold	-Exposure to saturated palmitic acids (250 µM, 500 µM, or 750 µM); -Exposure to unsaturated oleic acids (250 µM, 500 µM, or 750 µM)	-Palmitic acid exposure: lipid droplet sizes↑, insulin-sensitivity↑, basal lipolysis↑, secretion of pro-inflammatory cytokines which alter macrophage gene expression↑. -Oleic acid exposure: lipid droplet sizes↑, insulin-sensitivity↑.
	Taylor et al. (2020)[119]	mSVFs (with resident macrophages and monocytes maintained)	Seeded in 96-well ULA plates	-Exposure to saturated stearic acids (0.5mM); -Exposure to unsaturated oleic acids (0.5mM)	-Stearic acid exposure: lipolysis↑, a ratio of neutral to polar lipids↓. -Oleic acid exposure: lipolysis↑, levels of two polyunsaturated triglycerides↑, a ratio of neutral to polar lipids↓.
	Emont et al. (2015)[105]	Visceral and subcutaneous mSVFs	Cultured in collagen hydrogels	Collagen hydrogels support depot-specific characteristic maintenance	-SAT organoids: SAT markers (SHOX2 and TBX15)↑, thermogenic genes (CIDEA, COX7A1, DIO2, PPARGC1A, and PRDM16)↑. -VAT organoids: VAT markers (AGT and WT1)↑, cytokine genes (CCL2, CCL5, IL6, IL10, and TNFA)↑, secretion of cytokines (IL-6 and TNF-α) in response to LPS stimuli↑.
	Aubin et al. (2015)[97]	hADSCs	Superposition of 3 cell sheets	Exposure to TNF-α (10 ng/ml)	-Secretion of MCP-1↑, HGF↑, and NGF↑; NF-κB-dependent genes↑, genes implicated in NF-κB activation↑. -Functionally metabolic genes (GLUT4, FAS, and HSL)↓.
	Proulx et al. (2016)[95]	hADSCs and hMVECs	Superposition of 3 cell sheets	Exposure to TNF-α or IL-1β(10 ng/ml)	-Secretion of pro-inflammatory cytokines (MCP-1, IL-6, and Ang-1)↑. -Microvascular network formation↓.
	Abbott et al. (2018)[78]	Human liquified lipoaspirates from subjects with different BMI	Seeded into silk scaffolds	Exposure to TNF-α (10 ng/ml)	-Glucose uptake↑. -No significant differences in responsiveness of glucose uptake and lipid droplet sizes among WAOs derived from different subjects (BMI = 29, 30, 33, 36, 51 kg/m²).
	Harms et al. (2019)[43]	Visceral and subcutaneous adipocytes	Membrane mature adipocyte aggregate cultures	Co-cultured with mice macrophages (RAW264.7) and treated with LPS (10 ng/ml)	-Adipocytes: secretion of IL-6↑ and IL-8↑. -Macrophages: secretion of TNF-α↑ and IL-6↑.
	Taylor et al. (2020)[119]	mSVFs (with resident macrophages, mast cells, and other immune cells maintained)	Seeded in Nunclon Sphera 96-well ULA U-bottom plates	Exposure to LPS (100 ng/mL)	-Secretion of IL-6↑ and obesity-induced chemokine CCL2↑. -Lipidome changes found by mass spectrometry: diacylglycerol↓, cholesterol↑, no change in triglyceride fraction.
	Rajangam et al. (2016)[121]	hADSCs	Seeded in 96-well ULA plates	Immobilized FGF2 in well surfaces	Fibrosis-related genes (TGF-β1, αSMA, and Col I)↑, synthesis and accumulation of Col I↑, crosslinking of ECM components↑.
T2DM	Park et al. (2019)[83]	Mice 3L3-L1 preadipocytes	Suspended in alginate hydrogel mixture for 3D bioprinting	Co-cultured with mice macrophages (RAW264.7)	-Adipocytes: insulin-sensitivity markers (GLUT4 and pAKT)↓, a ratio of GLUT4 expressions in plasma membrane to cytosol↓, ISGU↓. -Macrophages: proliferation↑, pro-inflammatory cytokines (TNF-α and IL-1β)↑, F4/80↑, cytochrome C↑. -Levels of adipogenic markers comparable to 3D mono-culture.
	Park et al. (2020)[84]	hADSCs	Suspended in alginate hydrogel mixture for bioprinting of 3D beads	Loading hADSCs and mice macrophages (RAW264.7) in separate wells of 3D co-culture acrylic plates allowing cell interaction	-Insulin-sensitivity markers (GLUT4 and pAKT)↓, ISGU↓. -Macrophages proliferating from 1% to 15%. -Adipogenic differentiation capacity compared to 3D mono-culture.
	Choi et al. (2010)[116] Acosta et al. (2022)[38]	hADSCs and HUEVCs MVFs from T2DM and lean rats	Co-cultured in 3D silk scaffolds Embedded in fibrin hydrogels	High concentration of insulin (10 mM) exposure Fibrin hydrogels support subject-specific characteristic maintenance	-Triglyceride accumulation↑. -Glycerol release↓. -Db-MVF-derived WAOs: vessel structure size↓, vessel connections↓, ISGU↑, comparative levels of isoproterenol-stimulated lipolysis and OCR. -Db-MVF-derived BrAOs: vessel structure size↓, vessel connections↓, UCP1 expression↑, maximum respiration↑, spare capacity↑, comparative levels of ISGU and isoproterenol-stimulated lipolysis.
NAFLD	Slaughter et al. (2021)[104]	Primary human cardiac preadipocytes and primary human hepatocytes	Incorporated into two-chamber housing system	-Healthy plasma condition: post-prandial glucose (5 mM) and insulin (1 nM); -Diabetic plasma condition: post-prandial glucose (25 mM) and insulin (69 nM); -Pro-inflammatory plasma condition: TNF-α (10 µM); -Obese plasma condition: 45 µM BSA-conjugated palmitate and 65 µM oleate	-Steatosis↑ in diabetic medium with or without lipids and obese medium with and without TNF-α. -CYP3A4 activity↓ and adiponectin secretion↓ in proinflammatory medium alone and plus obese medium. -Leptin secretion↑ (slightly) and adiponectin to leptin ratio↓ in diabetic plus proinflammatory medium with and without lipids. -No significant changes in steatosis in pro-inflammatory medium and adiponectin secretion in diabetic and obese medium.

Alginate hydrogel mixture: containing 20 mg/mL alginate, 0.5 mg/mL gelatin, and 0.5 mg/mL Col I; Ang-1: angiotensinogen-converting enzyme 1; αSMA: α-smooth muscle actin; BMI: body mass index; BSA: bovine serum albumin; CIDEA: cell death-inducing DNA fragmentation factor alpha-like effector A; Col I: type I collagen; COX7A1: cytochrome c oxidase subunit 7A1; Db-MVF: microvascular fragments isolated from subcutaneous adipose tissues from diabetic rats; DIO2: iodothyronine deiodinase 2; ECM: extra cellular matrix; FAS: fatty acid synthase; GLUT4: glucose transporter 4; hADSC: human adipose-derived stem cell; HGF: hepatocyte growth factor; hMVEC: human microvascular

endothelial cell; HSL: hormone-sensitive lipase; HUEVC: human umbilical vein endothelial cells; IL: interleukin; ISGU: insulin-stimulated glucose uptake; LPS: lipopolysaccharide; MCP-1/CCL2: monocyte chemoattractant protein-1/C-C Motif Chemokine Ligand 2; mSVF: mice stromal vascular fraction; MVF: microvascular fragments; NF- κ B: nuclear factor kappa B; NGF: nerve growth factor; WAO: white adipose organoid; OCR: oxygen consumption rate; pAKT: AKT phosphorylation; PPAR γ C1A: peroxisome proliferator-activated receptor γ coactivator-1 α ; PRDM16: PR domain-containing 16; RANTES (CCL5): regulated-on-activation-normal-T-Cell-expressed-and secreted; SAT: subcutaneous adipose tissue; TGF- β : tumor growth factor beta; TNF- α : tumor necrosis factor-alpha; T2DM: type 2 diabetic mellitus; UCP1: uncoupled protein 1; ULA: ultra-low attachment; VAT: visceral adipose tissue; 3D: three-dimensional.

Table 2. Studies establishing adipose organoids as drug screening platforms for obesity-related metabolic diseases

Diseases	Studies	Sources	Methods	Efficiency validation	Screening drugs	Highlight results	In vivo validation
Obesity	Choi et al. (2022)[122]	mice 3T3-L1 preadipocytes and macrophages (RAW264.7)	-Suspended in alginate hydrogel mixture for bioprinting of 3D beads; -Tested in 96-well platforms	-Rosi: lipid accumulation \uparrow ; -GW9662: lipid accumulation \downarrow	178 compounds consisting of AMPK activators, PPAR γ agonists, and PPAR γ antagonists	-1 st hit: 7 compounds: adipogenesis \downarrow in 3D instead of 2D. -2 nd hit: 3 compounds: repetitive anti-adipogenic effects in 3D, adiponectin expression \uparrow ; Compound #71: pro-inflammatory cytokines (TNF- α , IL-6, and IL-1 β) \downarrow .	None
	Abbott et al. (2018)[78]	Human liquified lipoaspirates from ten subjects with different BMI	-Seeded into silk scaffolds; -Tested in 24-well platforms	None	AICAR (500 μ M): one of exercise mimetics	-Lipolysis \downarrow in only 3 of the 10 patient samples. -Responsiveness was not correlated with BMI (varied from 22, 23, 26, 30, 32, 32, 33, 33, 51 kg/m ²).	None
T2DM	Park et al. (2019)[83]	mice 3T3-L1 preadipocytes and macrophages (RAW264.7)	-Suspended in alginate hydrogel mixture for 3D bioprinting	Rosi: glucose uptake \uparrow , GLUT4 expression \uparrow , G6PD enzyme activity \downarrow	5 PPAR γ antagonists: GW9662, BADGE, SR202, FH535, and T0070907	-1 st hit: All 5 antagonists: lipogenesis-related genes and proteins (FABP4, ADIPOQ, PLIN, and PPAR γ 2) \downarrow . -2 nd hit: GW9662 (10 μ M): glucose uptake \uparrow , GLUT4 expression \uparrow , G6PD enzyme activity \downarrow .	C57BL/6 ^{ob/ob} mice orally administered GW9662 (300 mg/kg): -Body and fat weights \downarrow . -OGTT \uparrow , ITT \uparrow , HOMA-IR index \downarrow .
	Park et al. (2020)[84]	hADSCs and macrophages (RAW264.7)	-Suspended in alginate hydrogel mixture for bioprinting of 3D beads; -Loaded in separate wells of 3D co-culture acrylic plates allowing cell interaction	Metformin and Rosi: glucose uptake \uparrow , adiponectin secretion \uparrow	11 β -HSD1 inhibitors: KR-1 (mouse-potent enantiomer), KR-2 (human-potent enantiomer) KR-3 (racemic compound)	-1 st hit: KR-1 and KR-3: mouse 11 β -HSD1 \downarrow ; KR-2: human 11 β -HSD1 \downarrow . -2 nd hit: KR-1 and KR-3: glucose uptake \uparrow , GLUT4 expression \uparrow in mice-derived WAOs; KR-2 and KR-3: glucose uptake \uparrow , GLUT4 expression \uparrow in human-derived WAOs.	None
NAFLD	Slaughter et al. (2021)[104]	Primary human cardiac preadipocytes and primary human hepatocytes	Incorporated into two-chamber housing system	None	Metformin	Metformin (1mM) for a shortened 7-day treatment: -2D: Cell death. -3D: Steatosis \downarrow in diabetic, obese, diabetic plus obese, diabetic plus obese and proinflammatory medium.	Failure in clinical translation: The result dose is above physiological range in clinical application (1-50 μ M).

ADIPOQ: adiponectin; AICAR: 5-aminoimidazole-4-carboxamide-1- β -D-ribofuranoside; AMPK: adenosine monophosphate-activated protein kinase; BADGE: Bisphenol A diglycidyl ether; BMI: body mass index; FABP4: fatty acid binding protein 4; GLUT4: glucose transporter 4; GW9662: PPAR γ antagonist; G6PD: glucose-6-phosphate dehydrogenase; hADSC: human adipose-derived stem cells; HOMA-IR: Homeostatic Model Assessment for Insulin Resistance; IL: interleukin; ITT: insulin tolerance test; KR: compound synthesized at the Korean Research Institute of Chemical Technology; OGTT: oral glucose tolerance test; PLIN: perilipin; PPAR γ : peroxisome proliferator-activated receptor gamma; Rosi: rosiglitazone; TNF- α : tumor necrosis factor-alpha; WAO: white adipose organoid; 3D: three-dimensional; 11 β -HSD1: 11 β -hydroxysteroid dehydrogenase type 1.

Correspondingly, the transplantation of thermogenic adipocytes resulted in the alleviation of inflammation, evidenced by significantly reduced levels of TNF- α and IL-1 expression in adipose tissues and an increased ratio of adiponectin to leptin [65]. The host models included obese C57BL/6 mice fed with high-fat diet (HFD) [65,73], hyperglycemia non-obese diabetic/severe combined immunodeficiency (NOD/SCID) mice injected with streptozotocin (STZ) [64], and T2DM Rag1 $^{-/-}$ mice injected with STZ after 3-month HFD [36]. The ideal transplantation region encompassed hindlimb muscle [64,73] and kidney capsule [36] which provide a pro-browning microenvironment to avoid whitening. Wang et al. injected human BrAOs (with 1.25 million

adipocytes) derived from immortalized SVF-BATs into the kidney capsule of Rag1 $^{-/-}$ mice. After transplantation for 18 days, mice were fed with 3 months of HFD and injected with low-dose STZ (90 mg/kg) to establish obesity and T2DM models. Compared with the sham group, the transplantation group exhibited significant suppression in body weight and fat mass gains with UCP1 expression maintained in implants after transplantation for 5 months [36]. Besides, autologous reimplantation of BrAOs (0.2-0.3 grams) directly converted from SATs exhibited persistent brown-like phenotype after transplantation for 8 weeks, but its anti-obesity effect needs further evaluation (Figs. 4C-D and Table 3) [73].

Table 3. Studies establishing adipose organoids for transplantation to treat obesity-related metabolic diseases

Diseases	Studies	Sources	Methods	Amount	Host	Region	Highlight Results	Mechanisms
Obesity	Lee et al. (2017) [65]	hADSCs	Supplemented with transferrin (10 µg/ml), T3 (0.2 nM), and Rosi (100nM) to promote browning	1 million brown adipocytes/kg per 2 weeks for 10 weeks	C57BL/6j mice fed with 30-week HFD	Intraperitoneal	-Body weight↓, -TNF-α↓, IL-1↓, adiponectin-to-leptin ratio↑.	Unexplored
	Blumenfeld et al. (2018)[73]	Micro-WATs from HFD-fed C57BL/6 mice	Supplemented with T3 (250 nM), Rosi (1 µM), CL316243 (1 µM), and VEGF (25 ng/ml) for 3 weeks to promote ex vivo browning	0.2 ml BrAOs	HFD-fed C57BL/6 mice	Right rear hindlimb	-Body weight↓, fat mass↓ (significant at 15 weeks). -No significant differences in VO2 and EE at 1 week.	Unexplored
	Singh et al. (2020)[64]	hADSCs	Supplemented with transferrin (10 µg/ml), T3 (1 nM), Rosi (2 µM), Y-27632 (10 µM), and BMP7 (100ng/ml) to promote browning	2 million beige adipocytes	STZ-induced hyperglycemia NOD/SCID mice	Hindlimb muscle on both sides	-Body weight gain↓; -VO2↑, EE↑, core T↑.	Non-shivering thermogenesis to increase energy expenditure
	Wang et al. (2023)[36]	Immortalized hSVF-BATs	-PNIPAAm-PEG hydrogels promote uniformity of 3D BrAOs (100µm in diameter); -Supplemented with EBM-2, SB-431542 (5 µM), T3 (0.2 nM), and Rosi (1 µM) to enhance brown differentiation efficiency	1.25 million brown adipocytes in BrAO	Rag1 ^{-/-} mice fed with HFD for 3 months followed with low-dose STZ (90 mg/kg) injection	Kidney capsule	-Body weight gain↓, fat content↓. -UCP1 expression maintained for at least 5 months.	Unexplored
T2DM	Min et al. (2016)[34]	Human micro-SATs (1g)	-Embedded in Matrigels in EGM2-MV for angiogenesis; -Supplemented with EGM2-MV for 10-day differentiation and treated with Fsk (50 µM) for 7-day brown induction	10 million beige adipocytes	Glucose intolerant NSG mice through 2-week HFD treatment	Dorsal	-Fasting glucose level↓. -Glucose tolerance↑, glucose turnover↑ at 7 weeks.	Glucose turnover↑: -Extra glucose uptake of implants; -Neuroendocrine effects of the PSCK1-PENK-IL33 signaling pathway
	Lee et al. (2017) [65]	hADSCs	Supplemented with transferrin (10 µg/ml), T3 (0.2 nM), and Rosi (100nM) to promote browning	1 million brown adipocytes/kg per 2 weeks for 10 weeks	C57BL/6j mice fed with 30-week HFD	Intraperitoneal	-Fasting glucose level↓, insulin-sensitivity↑, glucose tolerance↑. -Glucose uptake in endogenous adipocytes and skeletal muscles↑. -Glucogenesis in livers↓. -Function and insulin-sensitivity of islets↑.	-GLUT4↑, PPARα↑ in endogenous adipocytes and skeletal muscles; -GLUT2↓, G6PC↓ in livers; -PPARα↑, PPARγ↑ in islets
	Tsagkaraki et al. (2021)[66]	-mSVF-WATs; -human preadipocytes[34]	Supplemented with Rosi (1 µM) and transfected with Cas9/ sgRNA RNPs to disrupt NRIP1 to promote browning	Brown adipocytes from a 1 × 150 mm fully confluent plate	NSG mice fed with HFD after transplantation	Subscapular	-Fasting glucose level↓ at 12 weeks. -Glucose intolerance↓ last over 15 weeks. -Maintenance of UCP1 expression for 16 weeks.	Unexplored
	Wang et al. (2020)[77]	hSVF-WATs	Supplemented with T3 (2 nM) and activate endogenous UCP1 by CRISPR-Cas9 to promote browning	15-20 million HUMBLE cells	Obese BALB/c athymic nude mice pretreated with 2-week HFD and continued HFD after transplantation	Thoracicsternum	-Preventive potential: glucose intolerance↓, insulin-resistance↓, insulin concentrations↓ at 4 weeks. -Long-term therapeutic potential: glucose intolerance↓, maintenance of UCP1 at 12 weeks.	NO produced by HUMBLE cells activated endogenous BATs: BAT-selective markers↑, glucose or fatty acid metabolism markers↑, glucose uptake↑
	Tsunao et al. (2015)[75]	Mice fibroblasts	Transduced with PRDM16, C/EBPB, and L-MYC and supplemented with T3 (1 nM) and Rosi (1 µM) to promote the direct conversion into dBA	dBAs from 2 confluent 100-mm dishes	C57BL/6 mice fed with HFD	Subcutaneous flank	Glucose tolerance↑, insulin-sensitivity↑ as early as 2 weeks after transplantation before weight loss.	Not secondary results of suppression of weight gain
	Zhang et al. (2020)[35]	hiPSCs	-Supplemented with NOGGIN (50 ng/ml), Fsk (5 µM), WNT3a (25 ng/ml), and BIO (2 µM) for paraxial	5 million brown adipocytes	Hyperglycemia NOD/SCID mice through 150 mg/kg STZ injection	Subcutaneous intrascapular	Non-fasting glucose level↓ over 7 days after transplantation, glucose intolerance↓.	GLUT1↑, glucose uptake↑, glycosis↑ of implants

Diseases	Studies	Sources	Methods	Amount	Host	Region	Highlight Results	Mechanisms
			mesoderm specification; -Supplemented with Rosi (2 μ M), BMP7 (100 ng/ml), T3 (1 nM), Y-27632 (10 μ M), and SB-431542 (10 μ M) to promote browning					
	Singh et al. (2020)[64]	hADSCs	Supplemented with transferrin (10 μ g/ml), T3 (1 nM), Rosi (2 μ M), Y-27632 (10 μ M) and BMP7 (100ng/ml) to promote browning	2 million beige adipocytes	Hyperglycemia NOD/SCID mice through 150 mg/kg STZ injection	-Subcutaneous intrascapular; -Hindlimb muscle on both sides	Non-fasting glucose level \downarrow over 5 days after transplantation, glucose intolerance \downarrow .	Glucose uptake \uparrow of implants
	Wang et al. (2023)[36]	Immortalized hSVF-BATs	-PNIPAAm-PEG hydrogels promote uniformity of 3D BrAOs (100 μ m in diameter); -Supplemented with EBM-2, SB-431542 (5 μ M), T3 (0.2 nM), and Rosi (1 μ M) to enhance brown differentiation efficiency	1.25 million brown adipocytes in BrAO	Rag1 ^{-/-} mice fed with HFD for 3 months followed with low-dose STZ (90 mg/kg) injection	Kidney capsule	Fasting glucose level \downarrow , glucose intolerance \downarrow , insulin-resistance \downarrow .	-Protect BATs, WATs, and livers from lipotoxicity; -Extra metabolic healthy adipokines (adiponectin, chemerin, and TGF- β) secreted by implants; -Endogenous adipokine secretion \uparrow
Dyslipidemia and NAFLD	Tsunao et al. (2015)[75]	-iPSCs derived from fibroblasts of T2DM KK-Ay mice; -fibroblasts from mice	iBAs: -Transduced with PRDM16; dBAs: -Transduced with PRDM16, C/EBPB, and L-MYC; -Supplemented with T3 (1 nM) and Rosi (1 μ M) to promote the direct conversion into dBAs	iBAs or dBAs from 2 confluent 100-mm dishes	-iBAs: KK-Ay T2DM mice; dBAs: KK-Ay T2DM mice, HFD-fed C57BL/6 mice	Subcutaneous flank	TC \downarrow , LDL cholesterol \downarrow , triglyceride \downarrow , phospholipid \downarrow , NEFA \downarrow , HDL/TC ratio \uparrow .	Unexplored
	Lee et al. (2017) [65]	hADSCs	Supplemented with transferrin (10 μ g/ml), T3 (0.2 nM) and Rosi (100nM) to promote browning	1 million brown adipocytes/kg per 2 weeks for 10 weeks	C57BL/6j mice fed with 30-week HFD	Intraperitoneal	-Dyslipidemia: TC \downarrow , TG \downarrow , HDL/TC ratio \uparrow . -NAFLD (Steatosis): lipid droplet accumulation \downarrow , hepatocellular ballooning \downarrow , liver function \uparrow (GPT \downarrow , AST \downarrow , Alb \uparrow). -NAFLD (NASH): inflammation \downarrow and fibrosis \downarrow in livers.	-Inflammation relief: pro-inflammatory cytokines (TNF- α and IL-4) \downarrow , anti-inflammatory cytokines (IL-1rn) \uparrow , F4/80 ⁺ macrophage infiltration \downarrow ; -Fibrosis relief: Col I \downarrow , ECM deposition \downarrow
	Tsagkaraki et al. (2021)[66]	mSVF-WATs; huma preadipocytes[34]	Supplemented with Rosi (1 μ M) and transfected with Cas9/ sgRNA RNPs to disrupt NRIP1 to promote browning	Brown adipocytes from a 1 \times 150 mm fully confluent plate	NSG mice fed with HFD after transplantation	Subscapular	Smaller and less pale liver with lipid droplet area \downarrow , number \downarrow , size \downarrow , TG \downarrow .	Genes related to fatty acid uptake (CD36) \downarrow and inflammation (MCP-1, TNF- α , and IL-1 β) \downarrow in livers

Alb: albumin; AST: aspartate transaminase; BAT: brown adipose tissue; BMP7: bone morphogenetic protein 7; BrAO: brown adipose organoid; CL316243: mice β 3 adrenoceptor agonist; Col I: type I collagen; dBA: fibroblasts directly converted into BAs by gene transduction; EBM-2: endothelial base medium 2; ECM: extra cellular matrix; EE: energy expenditure; EGM2-MV: endothelial cell growth medium-microvascular; Fsk: forskolin; GLUT: glucose transporter; GPT: glutamate pyruvate transaminase; G6PC: glucose-6-phosphatase; hADSC: human adipose-derived stem cell; HDL: high-density lipoprotein; HFD: high-fat diet; hSVF-BAT: human stromal vascular fragment from brown adipose tissue; HUMBLE: human brown-like; iBA: iPSC-derived embryoid bodies induced BA phenotypes; IL: interleukin; iPSC: induced pluripotent stem cell; LDL: low-density lipoprotein; MCP-1: monocyte chemoattractant protein-1; mSVF-WAT: mice stromal vascular fragment of white adipose tissue; NAFLD: non-alcoholic fatty liver disease; NASH: steatohepatitis; NEFA: non-essential fatty acid; NO: nitric oxide; NOD/SCID: non-obese diabetic/severe combined immunodeficiency; NSG: NOD-*scid* IL2 γ^{null} ; PENK: proenkephalin; PNIPAAm-PEG: poly(N-isopropylacrylamide)-poly(ethylene-glycol); PPAR α : peroxisome proliferator-activated receptor alpha; PPAR γ : peroxisome proliferator-activated receptor gamma; PRDM16: PR domain-containing 16; PSCK1: proprotein-converterase subtilisin/kexin type-1; Rag1^{-/-}: Rag1 knock-out; RNP: ribonucleoprotein; Rosi: rosiglitazone; SAT: subcutaneous adipose tissue; sgRNA: single-guide RNA; STZ: streptozotocin; T: temperature; TC: total cholesterol; TG: triglyceride; TGF- β : tumor growth factor beta; TNF- α : tumor necrosis factor-alpha; T2DM: type 2 diabetes mellitus; T3: 3,3',5-Triiodo-L-thyronine sodium salt; UCP1: uncoupled protein 1; VEGF: vascular endothelial growth factor; VO2: maximum volume of oxygen; WAT: white adipose tissue; 3D: three-dimensional.

4.2 Type 2 diabetes mellitus

According to the International Diabetes Federation in 2021, approximately 537 million people worldwide have diabetes, with 90% having T2DM [124]. The extensive prevalence of T2DM has positioned it as one of the most significant public health challenges [124,125]. Obesity stands out as a

crucial risk factor for T2DM [12,18,125]. Mechanistically, hypertrophic adipose tissues release pro-inflammatory cytokines and toxic lipolysis products that usually induce insulin-resistance in adipose tissues, livers, and skeletal muscles by inhibiting the IRS1-AKT-GLUT4 signaling pathway [32,117,126,127]. The prediabetic condition gradually progresses to T2DM as compensation for

insulin-resistance diminishes [128,129]. Common T2DM therapies include dietary and lifestyle interventions along with medications [13,129,130]. However, anti-diabetes drugs may cause adverse effects such as hypoglycemia, weight gain, and oedema [13,131]. For the discovery of innovative therapies targeting T2DM, WAOs co-cultured with macrophages are employed to mimic insulin-resistance for disease modeling and drug screening. Transplantation of BrAOs and BeAOs holds promise in treating T2DM by ameliorating glucose levels and improving insulin-resistance and glucose intolerance.

WAOs were co-cultured with mice macrophages in the alginate hydrogel mixture without impairing the adipogenic differentiation capacity to model insulin-resistance [83,84,112,122], characterized by lower p-AKT and GLUT4 expressions [83,84,122] and insulin-stimulated glucose uptake (ISGU) level^{94,95,12} than in the mono-culture system. Park et al. inflamed WAOs by mixing mice preadipocytes and macrophages in the alginate hydrogel mixture. Macrophages exhibited enhanced proliferation and activation in adipogenic differentiation medium, as evidenced by increased expression of pro-inflammatory TNF- α and IL-1 β , F4/80, and cytochrome C. The macrophage co-culture attenuated GLUT4 and pAKT expressions, the membrane-to-cytosol expression ratio of GLUT4, and ISGU [83]. Acosta et al. established patient-derived adipose organoids by seeding MVFs in fibrin hydrogels. The T2DM-derived adipose organoids showed less angiogenic capacity, but comparative lipolytic level and thermogenic potential relative to adipose organoids from lean mice (**Figure 4A** and **Table 1**) [38].

The co-culture system also served as a high-throughput screening platform for anti-T2DM drugs [83,84], validated by commercial drugs including rosiglitazone [83], and/or acarbose, metformin, and exendin-4 [84]. Park et al. assessed the effects of five PPAR γ antagonists on altering GLUT4 and p-AKT expressions and glucose-6-phosphate dehydrogenase activity. GW9662 exhibited optimal performance in improving insulin-resistance and enhancing glucose uptake [83]. However, interspecies differences in drug effects between mice-derived WAOs and human adipose tissues impede the clinical translation of screened drugs. Therefore, they further designed separate wells with cell interaction maintained to load human or mouse WAOs with mice macrophages to minimize interspecies errors. They employed 11 β -HSD1 inhibitors, including KR-1 (mouse-potent enantiomer), KR-2 (human-potent enantiomer), and KR-3 (racemic compound) for

validation. As a result, KR-2 and KR-3 better ameliorated insulin-resistance in human ADSC-derived WAOs, whereas KR-1 and KR-3 exhibited better effects on mice 3T3-L1-derived WAOs (**Figure 4B** and **Table 2**) [84].

Transplantation of beige and brown adipocytes as well as BrAOs decreased the glucose level [34–36,64–66,75] as well as improved glucose intolerance [34–36,64–66,75,77] and insulin-resistance [36,65,75,77]. Beige adipocytes [34] and brown adipocytes [65,66,75,77] were transplanted to obese C57B/L6 [65,75], NOD-*scid* IL2 γ ^{null} (NSG) [34,66] or BALB/c athymic nude mice fed with HFD [77]. Besides, beige adipocytes [64] and brown adipocytes [35] were transplanted to the subcutaneous intrascapular region [35,64] or hindlimb muscles [64] of hyperglycemia NOD/SCID mice with non-fasting glucose levels over 250 mg/dL after intraperitoneal injection of 150 mg/kg STZ [35,64]. The UCP1-dependent glucose metabolic benefit was not secondary to weight loss and persisted for over 16 weeks [66,75]. Apart from additional glucose uptake by the implant itself, implant-induced activation of endogenous BAT and an insulin-independent decrease in gluconeogenesis in livers also contributed to the decrease in blood glucose levels [34,65,77]. Transplantation also increased GLUT4 expression to improve insulin-resistance in adipocytes and skeletal muscles through PPAR α activation, as well as improved pancreatic function through PPAR α and PPAR γ activation [65].

Min et al. derived beige preadipocytes near the newly outgrowth capillaries of human micro-SATs (1g) embedded in Matrigels in the EGM medium. After adipogenic differentiation and 7-day Fsk treatment, beige adipocytes were derived and transplanted (10 million) to the dorsal region of glucose-intolerant NSG mice fed with 2-week HFD. Transplantation decreased fasting glucose levels while increasing glucose tolerance and turnover after 7 weeks. The increase in glucose turnover was partly attributed to the increased glucose uptake of implanted beige adipocytes along with the neuroendocrine effects of the PSCCK1-PENK-IL33 signaling pathway (**Figure 4D**) [34]. Through NR1P1 disruption by CRIPSR-Cas9, such preadipocytes were further induced to brown-like adipocytes which improved glucose metabolism over 12 weeks after transplantation [66]. Similarly, Wang et al. engineered human brown-like adipocytes from SVF-WATs by activating endogenous UCP1 via CRISPR-Cas9. They injected the brown-like adipocytes (15–20 million) into the thoracic-sternum region of obese BALB/c athymic nude mice pretreated with a 2-week HFD with continued HFD treatment after transplantation.

Transplantation showed both preventive and long-term therapeutic potentials of T2DM as evidenced by improvements in glucose metabolism at 4 weeks and 12 weeks after transplantation. Mechanistically, apart from implanted brown-like adipocytes, endogenous BAT activated by brown-like adipocyte-produced nitric oxide (NO) also contributed to glucose metabolic benefit (Table 3) [77].

Moreover, Wang et al. generated BrAOs from SVF-BATs in thermoreversible PNIPAAm-PEG hydrogels. They injected BrAO containing 1.25 million adipocytes into the kidney capsule of T2DM Rag1^{-/-} mice established via low-dose STZ (90 mg/kg) injection after 3-month HFD treatment. The fasting glucose level was reduced, accompanied by improved glucose intolerance and insulin-resistance. The safety of transplantation was confirmed as no tumor or non-adipose tissue was found. Moreover, transplantation also inhibited excessive lipid accumulation in endogenous BATs, WATs, and livers and improved the secretion of endogenous adipokines [36], which may also contribute to metabolic benefit as demonstrated in other studies (Figure 4C) [65,132]. Notably, PRDM16 transduction successfully induced iPSCs of T2DM KK-Ay mice into brown adipocytes, which reduced both serum and urine glucose levels of syngenic hosts after transplantation (Table 3) [75]. Besides, the medium of beige adipocytes derived from hiPSCs of T2DM patients increased insulin sensitivity and glucose uptake of the primary white adipocytes from the same patients [39]. These two studies showed the potential for autologous transplantation of BrAOs and BeAOs to treat T2DM.

4.3 Dyslipidemia and non-alcoholic fatty liver disease

Dyslipidemia, often secondary to obesity and T2DM, is characterized by elevated plasma levels of total cholesterol, LDL-cholesterol, or triglycerides, or reduced levels of HDL-cholesterol [133]. NAFLD has a global prevalence of 25% and affects over 80% of obese people [134–136]. NAFLD includes a disease continuum from steatosis to non-alcoholic steatohepatitis and even cirrhosis and hepatocellular carcinoma [136,137]. Mechanistically, hypertrophic adipose tissues usually induce increased lipolysis, inactivation of lipid metabolic enzymes, and lipotoxicity in livers [136,138]. Lifestyle and dietary interventions are crucial for managing dyslipidemia and NAFLD. However, long-term maintenance of lifestyle management poses challenges, necessitating the aid of inconvenient combined medications. Drugs like statins and fibrates can further treat dyslipidemia

while no therapy has been approved yet for NAFLD [13,136,139]. WAOs combined with organ-on-chip technology provide a platform to elucidate the role of adipose tissues in NAFLD progression and screen potential drugs [104,140]. Transplantation of brown adipocytes and BrAOs holds the potential to effectively treat dyslipidemia and NAFLD in a mono-modal manner.

Slaughter et al. developed the first human-on-chip model composed of human hepatocytes and human visceral adipocytes utilizing a serum-free, circulating medium to model healthy, diabetic, obese, and pro-inflammatory metabolic conditions. This model investigated the role of adipocyte lipolysis and insulin-resistance in NAFLD, and the crosstalk pattern of adipokines and cytokines exchanged between two organs. It also modeled the disparity of metformin efficacy on NAFLD between preclinical predictions and clinical results, demonstrating its potential for bridging the bench-to bedside gap in the evaluation of drug efficacy and dose regimens (Figures 4A–B and Tables 1–2) [104].

Transplantation of brown adipocytes [40,65,75] improved lipid metabolism profile in normal NOD/Shi-*scid* *IL2 γ* ^{null} mice [40] and alleviated dyslipidemia in obese C57BL/6 mice fed with HFD [65] and KK-Ay T2DM mice [75]. In detail, the serum lipid pattern was comparable to that of the normal diet group, exhibiting significantly lower levels of total cholesterol, triglyceride [40,65,75], LDL-cholesterol, phospholipid, and non-esterified fatty acids [75], as well as a significantly higher HDL/LDL ratio [65,75] compared to the control group. Furthermore, the olive oral tolerance test confirmed that brown adipocyte transplantation augmented resistance to oral lipid loading [40]. Besides, transplantation of brown adipocytes [65,66] demonstrated therapeutic effects on NAFLD in HFD-fed obese C57BL/6 [65] and NSG mice [66]. From a general perspective, the brown adipocyte group exhibited reduced liver weight and paleness. Histological analysis of the liver revealed decreased accumulation of lipid droplets and hepatocyte ballooning, which was further supported by the quantitative analysis of lipid droplet area, number, and size, as well as determination of liver triglyceride levels. Furthermore, the significantly lower serum levels of glutamate pyruvate transaminase and aspartate transaminase, along with elevated albumin levels indicated improved liver function. Moreover, hepatic inflammation was markedly alleviated with significant downregulation of expressions of pro-inflammatory genes such as MCP-1, TNF- α , IL-1 β , TNF- α , and IL-4, as well as upregulation of anti-inflammatory cytokine, IL1-rn, accompanied by

suppressed infiltration of F4/80 positive macrophages [65,66]. Tsagkaraki et al. generated brown adipocytes from SVF-WATs through NR1P1 disruption by CRISPR-Cas9 and transplanted them into the subscapular region of HFD-treated NSG mice. Livers were smaller and less pale with decreased area, number, and size of lipid droplets, as well as lower gene expressions of CD36 related to fatty acid uptake and pro-inflammatory TNF- α and IL-1 β after transplantation than control white groups [66]. Lee et al. administrated ADSC-derived brown adipocytes to C57BL/6 mice with steatosis and hepatomegaly through 30 weeks of HFD treatment. Lipid droplet accumulation and hepatocellular ballooning in livers were reversed, along with improved liver function [65]. Moreover, the long-term HFD also induced steatohepatitis characterized by inflammation and fibrosis. Transplantation significantly down-regulated expressions of pro-inflammatory TNF- α and IL-4, up-regulated expressions of anti-inflammatory IL-1 α , and repressed F4/80 positive macrophage infiltration for inflammation relief. Moreover, it showed therapeutic effects on liver fibrosis by reducing type I collagen expression and ECM deposition [65]. In addition to 2D brown adipocytes, transplantation of BraOs (1.25 million cells) from SVF-BATs to kidney capsules of T2DM mice also inhibited steatosis progression (Figure 4C and Table 3) [36].

5. Challenges and prospects

5.1 Establishment challenges and prospects

Adipose organoids are still in their infancy and have various establishment, bench-to bedside, and application challenges. There is currently no standardized stepwise strategy with designated intermediate stages like islet organoids to generate adipose organoids from PSCs [35,39,40,60,141]. Lineage tracing, RNA-seq, and ATAC-seq can further elucidate development processes in vivo, thereby guiding the stepwise induction in vitro [24,142,143]. Besides, beige adipocytes are always mistakenly recognized as brown ones. By characterizing intermediate stages, many 'brown adipocytes' actually undergoing the SplM stage were found to be beige ones [35,40,53,74,144]. Proteomics, transcriptomics, and open chromatin analyses are also utilized for identification by comparing with native adipose tissues [35,99,145].

Notably, 3D WAOs have been extensively established and applied to OMDs, whereas most researchers only generated 2D brown or beige adipocytes instead of 3D organoids. Considering the advantages of 3D, 3D fabrication techniques should be further applied to BeAO and BraO establishments.

However, current 3D adipose organoids still failed to fully recapitulate the structure and function of native adipose tissues [146]. One of the solutions is to characterize the disparities [35,99] and fill the gaps by improving source choices, induction recipes, and fabrication methods [66,77]. In addition to the aforementioned sources, adipogenic fibroblasts such as C3H10T1/2 MSCs [147,148] and 3T3-L1 preadipocytes [83,86,99,112,149], human dermal fibroblasts [75,150,151], and mature adipocytes [43] have also been applied. The progressively richer sources can better meet various needs of adipose organoids for applications. Additionally, the precise control of the application of small molecules at the appropriate stage is crucial. Notably, in the later stage of adipogenic differentiation, rosiglitazone is usually preserved [35,39,57,75], lipids are sometimes supplemented [35,57,91], while IBMX and dexamethasone are sometimes removed [36,38,60,92]. Considering the intimate relationship between circadian rhythm and adipose tissue homeostasis [152], particularly BAT [153], core circadian clock activators should be further applied to adipose organoids [154]. Meanwhile, vascularization, mechanical modification, and precise size control through microwells or hydrogels also promote maturation by improving adipokine secretion profile and metabolic activity [29,36,73].

Although once considered bland in morphology and function, adipose tissue is now recognized as heterogeneous, dynamic, and plastic. Over 60 subgroups of adipocytes, adipose stem and progenitor cells, preadipocytes, fibroblasts, ECs, and immune cells have been identified [155–157]. Therefore, the inclusion of ECs, neurons, and immune cells is crucial for generating mature adipose organoids and investigating intricate cell crosstalk [158]. Vascularization and immune cell incorporation in vitro have been well discussed in Section 3.4, whereas innervation has only been achieved after transplantation [36]. Notably, neuromesodermal progenitors have shown potential in self-organizing innervated mesoderm-derived organoids [159,160]. Besides, it is imperative to establish high-fidelity adipose organoids to elucidate the association of depot and subject heterogeneity with different physiologically or pathologically metabolic conditions. Mature adipocyte aggregate cultures, collagen and silk hydrogels, VAT-EC incorporation, and microfluidic systems can maintain depot-specific or subject-specific characteristics without impairing adipogenesis capacity, thereby facilitating the application of adipose organoids in disease modeling and drug screening [38,43,104,105,108,161].

Notably, adipose organoids also exhibited undesired or uncharacterized cell populations. This can be overcome by improving differentiation efficiency through optimized induction recipes, gene engineering techniques [64,66], and cell isolation during differentiation such as CD29 for thermogenic preadipocytes [40,57,81]. Many studies lacked quantification of differentiation efficiency. The differentiation efficiency of white adipocytes is usually quantified by lipid droplet staining. For beige and brown adipocytes, UCP1 expression levels should be additionally characterized by immunostaining or flow cytometry [35,64]. Notably, flow cytometry may underestimate the efficiency due to the high buoyancy of adipocytes [35]. Additionally, batch-to-batch variations in viability, size, differentiation efficiency, and functionality pose challenges in high-throughput research and undermine result credibility [41]. Therefore, standardization of establishment protocols is necessary [36].

5.2 Bench-to-bedside challenges and prospects

Although hiPSC-derived adipose organoids show great promise in personalized medicine, their tumorigenicity which requires a rigorous evaluation before transplantation blocks further clinical application. Recently, a transient-naive-treatment reprogramming method has shown the potential to overcome this limitation [162]. In addition, vascularization, innervation, and minimal immune response are imperative for the long-term survival of functional implants. Besides the aforementioned methods, embedding a catheter at the transplant site directly promoted vascularization in vivo [163]. Notably, current transplantations have always been conducted in immunodeficiency or immunocompromised mice which is not applicable to humans. The employment of CRISPR-Cas9 to eliminate human leukocyte antigen expressions and ex vivo interferon- γ stimulation to induce endogenous PD-L1 expressions show promise in solving immune issues [143,164]. Furthermore, although scaffold-based strategies show advantages in uniformity for high-throughput research, ethical concerns render their further clinical translation. To overcome this, enzyme digestion for scaffold removal and biosafe hydrogels such as thermoreversible and human-derived hydrogels have been applied [36,107], as well as droplet emulsion microfluidic which generates thousands of size-controlled (250-450 μm in diameter) micro-organospheres [165]. For further clinical translation, attention should also be given to serum-free medium to avoid xenogeneic contamination and hydrogels supporting long-term preservation [36,64].

It is noteworthy that transplantation of thermogenic BrAOs and BeAOs shows great potential for the treatment of OMDs. However, it is important to achieve long-term therapeutic effects on metabolic improvement considering the time and effort cost of in vitro construction and in vivo invasive procedures. Although previous in vivo experiments have demonstrated efficacy up to 180 days [36], many researchers have overlooked the importance of emphasizing and exploring long-term efficacy, often limiting observations to only 1-2 weeks after transplantation while disregarding the potential whitening of thermogenic adipose grafts in vivo [35,64]. To address this issue, it is crucial to first clarify the nature of brown and beige adipose tissues. BAT, originating from paraxial mesoderm, is a stable thermogenic adipose tissue, whereas beige adipose tissue, emerging from WAT under stimuli, is unstable. Therefore, further elucidation of the in vivo developmental trajectory of BAT is imperative for facilitating the construction of authentic BrAOs in vitro instead of BeAOs which go whitening without browning stimuli in vivo after transplantation. In addition, the current studies that achieved long-term effects are those that transplanted BrAOs rather than brown adipocytes. This may be attributed to the fact that organoids can better facilitate the cell-cell and cell-ECM interactions to support thermogenic phenotype maintenance. In addition, considering sites for transplantation is also noteworthy as regions that naturally distribute thermogenic adipose tissues such as interscapular regions may provide a more favorable microenvironment to avoid whitening.

5.3 Application challenges and prospects

WAOs have been mainly applied to disease modeling and drug screening of OMDs. Considering the metabolic healthy adipokine secretion, it should be potential for OMD treatment and did reduce triglyceride levels and improve lipid intolerance [40]. Nevertheless, it was also reported to induce glucose intolerance and insulin-resistance [40]. Therefore, further studies are required to explore the therapeutic potential of WAOs. BrAOs and BeAOs have been mainly used for transplantation to treat OMDs. However, many studies only listed therapeutic phenomena without elucidation of mechanisms. In addition to the direct effects of implants, their effects on other organs such as endogenous WATs and BATs, livers, skeletal muscles, and central nervous systems possibly through batokines [166] may also contribute to the metabolic benefits [167]. Additionally, BeAOs and BrAOs should be further employed in high-throughput screening of novel browning molecules [43,64,69] to enhance ex vivo browning

efficiency for transplantation and promote in vivo white-to-beige transition after oral administration [69]. Notably, inosine secretion from apoptotic brown adipocytes [168] and damaged mitochondria removal of macrophages [169] were reported to promote thermogenesis in BATs. Therefore, investigations on cell crosstalk in adipose organoids are required. In addition, adipose organoids should be further applied to cirrhosis, hepatocellular carcinoma, and cardiovascular diseases [170], as well as systematic inflammation diseases such as osteoarthritis [113].

6. Conclusions

Translational OMD research is significantly hampered by the lack of accurate and reliable in vitro models that can faithfully replicate human physiology and pathology. Meanwhile, transplantation of brown and beige adipose tissues to treat OMD is restricted by their scarcity in vivo. Adipose organoids derived from PSCs, ADSCs, SVF-WATs, SVF-BATs, and micro-WATs provide a promising platform for unraveling underlying mechanisms and developing potential treatments of OMDs. Specifically, WAOs were mainly used for disease modeling and drug screening, while BeAOs and BraAO showed promise in increasing energy expenditure and improving lipid and glucose metabolism upon transplantation. Various scaffold-free and scaffold-based 3D techniques, along with strategies to promote vascularization and immune cell incorporation, have been extensively employed in adipose organoids; however, adipose organoids still fail to fully recapitulating the intricate structure and function of adipose tissues in vivo. In fact, advancements are required to improve the maturity and heterogeneity during establishment, address immune rejection challenges and safety concerns associated with transplantation, as well as expand applications in OMDs for further progress. The continued development of adipose organoids will be a milestone in comprehending and treating OMDs.

Abbreviations

3D: three-dimensional; BAT: brown adipose tissue; BeAO: beige adipose organoid; BraAO: brown adipose organoid; C/EBP α : CCAAT/enhancer binding protein α ; dECM: decellularized extracellular matrix; EB: embryonic body; EC: endothelial cell; ECM: extracellular matrix; ELP: elastin-like polypeptide; GelMA/HAMA: methacrylate gelatin and hyaluronic acid; HFD: high-fat diet; IBMX: 3-Isobutyl-1-methylxanthine; ISGU: insulin-stimulated glucose uptake; LPS: lipopolysaccharide; MSC: mesenchymal stem cell; MVF: microvascular fragment; NAFLD: non-alcoholic fatty liver disease;

NOD/SCID: non-obese diabetic/severe combined immunodeficiency; NSG: NOD-*scid* *IL2r γ ^{null}*; OCR: oxygen consumption rate; OMD: obesity-related metabolic disease; PEI: polyethyleneimine; PLGA: poly(lactic-co-glycolic acid); PNIPAAm-PEG: poly(N-isopropylacrylamide)-poly(ethylene-glycol); PPAR γ : peroxisome proliferator-activated receptor γ ; SAT: subcutaneous adipose tissue; SplM: splanchnic mesoderm; SVF: stromal vascular fragment; STZ: streptozotocin; SVF-WAT: stromal vascular fragment from white adipose tissue; T2DM : type 2 diabetes mellitus; T3: triiodothyronine; UCP1: uncoupling protein 1; VAT: visceral adipose tissue; WAO: white adipose organoid.

Acknowledgements

Funding

This research was supported by grants from the National Natural Science Foundation of China (82372535), Shanghai Clinical Research Center of Plastic and Reconstructive Surgery supported by Science and Technology Commission of Shanghai Municipality (22MC1940300), and the Shanghai Municipal Key Clinical Specialty (shslczdzk00901).

Author contributions

All authors read and approved the final version of the manuscript. R.L.H. and Q.L. designed the study and provided guidance. X.L., Y.Y., and J.Y. analyzed the data. X.L. and R.L.H. prepared the figures and wrote the manuscript with assistance from Y.Y., J.Y., and Q.L. All authors confirm that they have full access to all study data and accept responsibility for publication submission.

Competing Interests

The authors have declared that no competing interest exists.

References

- González-Muniesa P, Martínez-González M-A, Hu FB, Després J-P, Matsuzawa Y, Loos RJF, et al. Obesity. Nat Rev Dis Primer. 2017; 3: 17034.
- [Internet] WHO. Obesity and overweight. Revised 9 June 2021. <https://www.who.int/news-room/fact-sheets/detail/obesity-and-overweight>
- [Internet] WHO. World Obesity Day 2022 - Accelerating action to stop obesity. Revised 4 March 2022. <https://www.who.int/news/item/04-03-2022-world-obesity-day-2022-accelerating-action-to-stop-obesity>
- [Internet] WHO. Obesity. <https://www.who.int/health-topics/obesity>
- Khan S, Luck H, Winer S, Winer DA. Emerging concepts in intestinal immune control of obesity-related metabolic disease. Nat Commun. 2021; 12: 2598.
- Friedman SL, Neuschwander-Tetri BA, Rinella M, Sanyal AJ. Mechanisms of NAFLD development and therapeutic strategies. Nat Med. 2018; 24: 908–22.
- Hu W, Lazar MA. Modelling metabolic diseases and drug response using stem cells and organoids. Nat Rev Endocrinol. 2022; 18: 744–59.
- Zhao G-N, Tian Z-W, Tian T, Zhu Z-P, Zhao W-J, Tian H, et al. TMBIM1 is an inhibitor of adipogenesis and its depletion promotes adipocyte

- hyperplasia and improves obesity-related metabolic disease. *Cell Metab.* 2021; 33: 1640-1654.e8.
9. Geng L, Lam KSL, Xu A. The therapeutic potential of FGF21 in metabolic diseases: from bench to clinic. *Nat Rev Endocrinol.* 2020; 16: 654-67.
 10. Blüher M. Obesity: global epidemiology and pathogenesis. *Nat Rev Endocrinol.* 2019; 15: 288-98.
 11. Lister NB, Baur LA, Felix JF, Hill AJ, Marcus C, Reinehr T, et al. Child and adolescent obesity. *Nat Rev Dis Primer.* 2023; 9: 24.
 12. Perdomo CM, Cohen RV, Sumithran P, Clément K, Frühbeck G. Contemporary medical, device, and surgical therapies for obesity in adults. *Lancet Lond Engl.* 2023; 401: 1116-30.
 13. Ferguson D, Finck BN. Emerging therapeutic approaches for the treatment of NAFLD and type 2 diabetes mellitus. *Nat Rev Endocrinol.* 2021; 17: 484-95.
 14. Marsee A, Roos FJM, Verstegen MMA, Gehart H, De Koning E, Lemaigre F, et al. Building consensus on definition and nomenclature of hepatic, pancreatic, and biliary organoids. *Cell Stem Cell.* 2021; 28: 816-32.
 15. Zhao Z, Chen X, Dowbaj AM, Slijkic A, Bratlie K, Lin L, et al. Organoids. *Nat Rev Methods Primer.* 2022; 2: 1-21.
 16. Hofer M, Lutolf MP. Engineering organoids. *Nat Rev Mater.* 2021; 6: 402-20.
 17. Kratochvil MJ, Seymour AJ, Li TL, Paşca SP, Kuo CJ, Heilshorn SC. Engineered materials for organoid systems. *Nat Rev Mater.* 2019; 4: 606-22.
 18. Piché M-E, Tchernof A, Després J-P. Obesity phenotypes, diabetes, and cardiovascular diseases. *Circ Res.* 2020; 126: 1477-500.
 19. Shamsi F, Wang C-H, Tseng Y-H. The evolving view of thermogenic adipocytes - ontogeny, niche and function. *Nat Rev Endocrinol.* 2021; 1-19.
 20. Kislev N, Izgilov R, Adler R, Benayahu D. Exploring the cell stemness and the complexity of the adipose tissue niche. *Biomolecules.* 2021; 11: 1906.
 21. Cohen P, Kajimura S. The cellular and functional complexity of thermogenic fat. *Nat Rev Mol Cell Biol.* 2021; 22: 393-409.
 22. Carobbio S, Guénant A-C, Samuelson I, Bahri M, Vidal-Puig A. Brown and beige fat: From molecules to physiology and pathophysiology. *Biochim Biophys Acta BBA - Mol Cell Biol Lipids.* 2019; 1864: 37-50.
 23. Ghaben AL, Scherer PE. Adipogenesis and metabolic health. *Nat Rev Mol Cell Biol.* 2019; 20: 242-58.
 24. Wang W, Seale P. Control of brown and beige fat development. *Nat Rev Mol Cell Biol.* 2016; 17: 691-702.
 25. Vera M, Pieters, Saïfedine T, Rjaïbi, Kanwaldeep Singh, Li NT, Safwat T Khan, Altalhi W, et al. A three-dimensional human adipocyte model of fatty acid-induced obesity. 2022; 14(4).
 26. Klingelutz AJ, Gourronc FA, Chaly AL, Wadkins DA, Burand AJ, Markan KR, et al. Scaffold-free generation of uniform adipose spheroids for metabolism research and drug discovery. *Sci Rep.* 2018; 8: 523-523.
 27. Aubin K, Vincent C, Proulx M, Mayrand D, Fradette J. Creating capillary networks within human engineered tissues: Impact of adipocytes and their secretory products. *Acta Biomater.* 2015; 11: 333-45.
 28. Abbott RD, Wang RY, Reagan MR, Chen Y, Borowsky FE, Zieba A, et al. The use of silk as a scaffold for mature, sustainable unilocular adipose 3D tissue engineered systems. *Adv Healthc Mater.* 2016; 5: 1667-77.
 29. Kuss M, Kim J, Qi D, Wu S, Lei Y, Chung S, et al. Effects of tunable, 3D-bioprinted hydrogels on human brown adipocyte behavior and metabolic function. *Acta Biomater.* 2018; 71: 486-95.
 30. Strobel HA, Gerton T, Hoying JB. Vascularized adipocyte organoid model using isolated human microvessel fragments. *Biofabrication.* 2021; 13: 035022.
 31. Paek J, Park SE, Lu Q, Park K-T, Cho M, Oh JM, et al. Microphysiological engineering of self-assembled and perfusable microvascular beds for the production of vascularized three-dimensional human microtissues. *ACS Nano.* 2019; 13: 7627-43.
 32. Kusminski CM, Bickel PE, Scherer PE. Targeting adipose tissue in the treatment of obesity-associated diabetes. *Nat Rev Drug Discov.* 2016; 15: 639-60.
 33. Inagaki T, Sakai J, Kajimura S. Transcriptional and epigenetic control of brown and beige adipose cell fate and function. *Nat Rev Mol Cell Biol.* 2016; 17: 480-95.
 34. Min SY, Kady J, Nam M, Rojas-Rodriguez R, Berkenwald A, Kim JH, et al. Human 'brite/beige' adipocytes develop from capillary networks, and their implantation improves metabolic homeostasis in mice. *Nat Med.* 2016; 22: 312-8.
 35. Zhang L, Avery J, Yin A, Singh AM, Cliff TS, Yin H, et al. Generation of functional brown adipocytes from human pluripotent stem cells via progression through a paraxial mesoderm state. *Cell Stem Cell.* 2020; 27: 784-797.e11.
 36. Wang O, Han L, Lin H, Tian M, Zhang S, Duan B, et al. Fabricating 3-dimensional human brown adipose microtissues for transplantation studies. *Bioact Mater.* 2023; 22: 518-34.
 37. Tseng Y-H, Kokkotou E, Schulz TJ, Huang TL, Winnay JN, Taniguchi CM, et al. New role of bone morphogenetic protein 7 in brown adipogenesis and energy expenditure. *Nature.* 2008; 454: 1000-4.
 38. Acosta FM, Stojkova K, Zhang J, Garcia Huitron EI, Jiang JX, Rathbone CR, et al. Engineering functional vascularized beige adipose tissue from microvascular fragments of models of healthy and type II diabetes conditions. *J Tissue Eng.* 2022; 13: 20417314221109337.
 39. Su S, Guntur AR, Nguyen DC, Fakory SS, Doucette CC, Leech C, et al. A renewable source of human beige adipocytes for development of therapies to treat metabolic syndrome. *Cell Rep.* 2018; 25: 3215-3228.e9.
 40. Nishio M, Yoneshiro T, Nakahara M, Suzuki S, Saeki K, Hasegawa M, et al. Production of functional classical brown adipocytes from human pluripotent stem cells using specific hemopoietin cocktail without gene transfer. *Cell Metab.* 2012; 16(3):394-406.
 41. Xue R, Lynes MD, Dreyfuss JM, Shamsi F, Schulz TJ, Zhang H, et al. Clonal analyses and gene profiling identify genetic biomarkers of the thermogenic potential of human brown and white preadipocytes. *Nat Med.* 2015; 21: 760-8.
 42. Robledo F, González-Hodar L, Tapia P, Figueroa A-M, Ezquer F, Cortés V. Spheroids derived from the stromal vascular fraction of adipose tissue self-organize in complex adipose organoids and secrete leptin. *Stem Cell Res Ther.* 2023; 14(1): 70.
 43. Harms MJ, Li Q, Lee S, Zhang C, Kull B, Hallén S, et al. Mature human white adipocytes cultured under membranes maintain identity, function, and can transdifferentiate into brown-like adipocytes. *Cell Rep.* 2019; 27: 213-25.
 44. Zhang Y, Zhang Y, Dong Y, Chen T, Xu G. Generation of functional fat organoid from rat superficial fascia. *Adipocyte.* 2022; 11: 287-300.
 45. Yang JP, Anderson AE, McCartney A, Ory X, Ma G, Pappalardo E, et al. Metabolically active three-dimensional brown adipose tissue engineered from white adipose-derived stem cells. *Tissue Eng Part A.* 2017; 23: 253-62.
 46. Loh KM, Chen A, Koh PW, Deng TZ, Sinha R, Tsai JM, et al. Mapping the pairwise choices leading from pluripotency to human bone, heart, and other mesoderm cell types. *Cell.* 2016; 166: 451-67.
 47. Chal J, Pourquié O. Making muscle: skeletal myogenesis *in vivo* and *in vitro*. *Development.* 2017; 144: 2104-22.
 48. Ahfeldt T, Schinzel RT, Lee Y-K, Hendrickson D, Kaplan A, Lum DH, et al. Programming human pluripotent stem cells into white and brown adipocytes. *Nat Cell Biol.* 2012; 14: 209-19.
 49. Schreiber I, Dörpholz G, Ott C-E, Kragesteen B, Schanze N, Lee C, et al. BMPs as new insulin sensitizers: Enhanced glucose uptake in mature 3T3-L1 adipocytes via PPAR γ and GLUT4 upregulation. *Sci Rep.* 2017; 7(1):17192.
 50. Guilherme A, Yenilmez B, Bedard AH, Henriques F, Liu D, Lee A, et al. Control of adipocyte thermogenesis and lipogenesis through β 3-adrenergic and thyroid hormone signal integration. *Cell Rep.* 2020; 31: 107598.
 51. Overby H, Yang Y, Xu X, Wang S, Zhao L. Indomethacin promotes browning and brown adipogenesis in both murine and human fat cells. *Pharmacol Res Perspect.* 2020; 8: e00592.
 52. Al-Ali MM, Khan AA, Fayyad AM, Abdallah SH, Khattak MNK. Transcriptomic profiling of the telomerase transformed mesenchymal stromal cells derived adipocytes in response to rosiglitazone. *BMC Genom Data.* 2022; 23(1): 17.
 53. Hafner A-L, Contet J, Ravaut C, Yao X, Villageois P, Suknutha K, et al. Brown-like adipose progenitors derived from human induced pluripotent stem cells: Identification of critical pathways governing their adipogenic capacity. *Sci Rep.* 2016; 6: 32490.
 54. Kim N-J, Baek J-H, Lee J, Kim H, Song J-K, Chun K-H. A PDE1 inhibitor reduces adipogenesis in mice via regulation of lipolysis and adipogenic cell signaling. *Exp Mol Med.* 2019; 51: 1-15.
 55. Khalilpourfarshbafi M, Gholami K, Murugan DD, Abdul Sattar MZ, Abdullah NA. Differential effects of dietary flavonoids on adipogenesis. *Eur J Nutr.* 2019; 58(1):5-25.
 56. Roh HC, Kumari M, Taleb S, Tenen D, Jacobs C, Lyubetskaya A, et al. Adipocytes fail to maintain cellular identity during obesity due to reduced PPAR γ activity and elevated TGF β -SMAD signaling. *Mol Metab.* 2020; 42: 101086.
 57. Carobbio S, Guénant A-C, Bahri M, Rodriguez-Fdez S, Honig F, Kamzolas I, et al. Unraveling the developmental roadmap toward human brown adipose tissue. *Stem Cell Rep.* 2021; 16: 641-55.
 58. Mandl M, Viertler HP, Hatzmann FM, Brucker C, Großmann S, Waldegger P, et al. An organoid model derived from human adipose stem/progenitor cells to study adipose tissue physiology. *Adipocyte.* 2022; 11: 164-74.

59. Wang B, Fu X, Liang X, Deavala JM, Wang Z, Zhao L, et al. Retinoic acid induces white adipose tissue browning by increasing adipose vascularity and inducing beige adipogenesis of PDGFR α + adipose progenitors. *Cell Discov.* 2017; 3: 17036.
60. Guénant A-C, Briand N, Capel E, Dumont F, Morichon R, Provost C, et al. Functional human beige adipocytes from induced pluripotent stem cells. *Diabetes.* 2017; 66: 1470–8.
61. Kong X, Banks A, Liu T, Kazak L, Rao RR, Cohen P, et al. IRF4 is a key thermogenic transcriptional partner of PGC-1 α . *Cell.* 2014; 158: 69–83.
62. Ohno H, Shinoda K, Spiegelman BM, Kajimura S. PPAR γ agonists induce a white-to-brown fat conversion through stabilization of PRDM16 protein. *Cell Metab.* 2012;15(3):395–404.
63. Shinoda K, Luijten IHN, Yutaka Hasegawa, Hasegawa Y, Hong H, Sonne SB, et al. Genetic and functional characterization of clonally derived adult human brown adipocytes. *Nat Med.* 2015; 21: 389–94.
64. Singh AM, Zhang L, Avery J, Yin A, Du Y, Wang H, et al. Human beige adipocytes for drug discovery and cell therapy in metabolic diseases. *Nat Commun.* 2020; 11: 2758.
65. Lee C-W, Hsiao W-T, Lee OK-S. Mesenchymal stromal cell-based therapies reduce obesity and metabolic syndromes induced by a high-fat diet. *Transl Res.* 2017; 182: 61–74.e8.
66. Tsagkaraki E, Nicoloso SM, DeSouza T, Solivan-Rivera J, Desai A, Lifshitz LM, et al. CRISPR-enhanced human adipocyte browning as cell therapy for metabolic disease. *Nat Commun.* 2021; 12: 6931.
67. Liu S, Shen S, Yan Y, Sun C, Lu Z, Feng H, et al. Triiodothyronine (T3) promotes brown fat hyperplasia via thyroid hormone receptor α mediated adipocyte progenitor cell proliferation. *Nat Commun.* 2022; 13: 3394.
68. Bocco BM, Louzada RA, Silvestre DH, Santos MC, Anne-Palmer E, Rangel IF, et al. Thyroid hormone activation by type 2 deiodinase mediates exercise-induced peroxisome proliferator-activated receptor- γ coactivator-1 α expression in skeletal muscle. *J Physiol.* 2016; 594: 5255–69.
69. Qiu Y, Sun Y, Xu D, Yang Y, Liu X, Wei Y, et al. Screening of FDA-approved drugs identifies suturent as a modulator of UCP1 expression in brown adipose tissue. *EBioMedicine.* 2018; 37: 344–355.
70. Wang X, You L, Cui X, Li Y, Wang X, Xu P, et al. Evaluation and optimization of differentiation conditions for human primary brown adipocytes. *Sci Rep.* 2018; 8: 5304–5304.
71. Mullur R, Liu Y-Y, Brent GA. Thyroid hormone regulation of metabolism. *Physiol Rev.* 2014; 94: 355–82.
72. Barquissau V, Beuzelin D, Pisani DF, Beranger GE, Mairal A, Montagner A, et al. White-to-brite conversion in human adipocytes promotes metabolic reprogramming towards fatty acid anabolic and catabolic pathways. *Mol Metab.* 2016;5(5):352–365.
73. Blumenfeld NR, Kang HJ, Fenzl A, Song Z, Chung JJ, Singh R, et al. A direct tissue-grafting approach to increasing endogenous brown fat. *Sci Rep.* 2018; 8: 7957.
74. Mohsen-Kanson T, Hafner A-L, Wdziekonski B, Takashima Y, Villageois P, Carrière A, et al. Differentiation of human induced pluripotent stem cells into brown and white adipocytes: Role of Pax3. *Stem Cells.* 2014; 32: 1459–67.
75. Tsunao Kishida, Kishida T, Ejima A, Yamamoto K, Tanaka S, Yamamoto T, et al. Reprogrammed functional brown adipocytes ameliorate insulin resistance and dyslipidemia in diet-induced obesity and type 2 diabetes. *Stem Cell Rep.* 2015; 5: 569–81.
76. Zhang K, Song L, Wang J, Yan S, Li G, Cui L, et al. Strategy for constructing vascularized adipose units in poly(l-glutamic acid) hydrogel porous scaffold through inducing in-situ formation of ASCs spheroids. *Acta Biomater.* 2017; 51: 246–57.
77. Wang C-H, Lundh M, Fu A, Kriszt R, Huang TL, Lynes MD, et al. CRISPR-engineered human brown-like adipocytes prevent diet-induced obesity and ameliorate metabolic syndrome in mice. *Sci Transl Med.* 2020; 12: eaaz8664.
78. Abbott RD, Borowsky FE, Alonzo CA, Zieba A, Georgakoudi I, Kaplan DL. Variability in responses observed in human white adipose tissue models. *J Tissue Eng Regen Med.* 2018; 12: 840–7.
79. Lau FH, Vogel K, Luckett JP, Hunt M, Meyer A, Rogers CL, et al. Sandwiched white adipose tissue: A microphysiological system of primary human adipose tissue. *Tissue Eng Part C Methods.* 2018; 24: 135–45.
80. Bahmad HF, Daouk R, Azar J, Sapudom J, Teo JCM, Abou-Kheir W, et al. Modeling adipogenesis: Current and future perspective. *Cells.* 2020; 9: 2326.
81. Shen JX, Couchet M, Dufau J, de Castro Barbosa T, Ulbrich MH, Helmstädter M, et al. 3D adipose tissue culture links the organotypic microenvironment to improved adipogenesis. *Adv Sci (Weinh).* 2021; 8: e2100106.
82. Gibler P, Gimble J, Hamel K, Rogers E, Henderson M, Wu X, et al. Human adipose-derived stromal/stem cell culture and analysis methods for adipose tissue modeling in vitro: A systematic review. *Cells.* 2021; 10: 1378.
83. Park SB, Lee SY, Jung WH, Lee J, Jeong HG, Hong J, et al. Development of in vitro three-dimensional co-culture system for metabolic syndrome therapeutic agents. *Diabetes Obes Metab.* 2019; 21: 1146–57.
84. Park SB, Koh B, Jung WH, Choi KJ, Na YJ, Yoo HM, et al. Development of a three-dimensional in vitro co-culture model to increase drug selectivity for humans. *Diabetes Obes Metab.* 2020; 22: 1302–15.
85. Unser AM, Tian Y, Xie Y. Opportunities and challenges in three-dimensional brown adipogenesis of stem cells. *Biotechnol Adv.* 2015; 33: 962–79.
86. Turner PA, Tang Y, Weiss SJ, Janorkar AV. Three-dimensional spheroid cell model of *in vitro* adipocyte inflammation. *Tissue Eng Part A.* 2015; 21: 1837–47.
87. Labriola NR, Sadick JS, Morgan JR, Mathiowitz E, Darling EM. Cell mimicking microparticles influence the organization, growth, and mechanophenotype of stem cell spheroids. *Ann Biomed Eng.* 2018; 46: 1146–59.
88. Al-Ghadban S, Pursell IA, Diaz ZT, Herbst KL, Bunnell BA. 3D spheroids derived from human lipedema ASCs demonstrated similar adipogenic differentiation potential and ECM remodeling to non-lipedema ASCs in vitro. *Int J Mol Sci.* 2020; 21: 8350.
89. Shen K, Vesey DA, Hasnain SZ, Zhao K-N, Wang H, Johnson DW, et al. A cost-effective three-dimensional culture platform functionally mimics the adipose tissue microenvironment surrounding the kidney. *Biochem Biophys Res Commun.* 2020; 522: 736–42.
90. Di Stefano AB, Grisafi F, Castiglia M, Perez A, Montesano L, Gulino A, et al. Spheroids from adipose-derived stem cells exhibit an miRNA profile of highly undifferentiated cells. *J Cell Physiol.* 2018; 233: 8778–89.
91. Muller S, Ader I, Creff J, Leménager H, Achard P, Casteilla L, et al. Human adipose stromal-vascular fraction self-organizes to form vascularized adipose tissue in 3D cultures. *Sci Rep.* 2019; 9: 7250–7250.
92. Turner PA, Gurumurthy B, Bailey JL, Elks CM, Janorkar AV. Adipogenic differentiation of human adipose-derived stem cells grown as spheroids. *Process Biochem Barking Lond Engl.* 2017; 59: 312–20.
93. Ohguro H, Ida Y, Hikage F, Umetsu A, Ichioka H, Watanabe M, et al. STAT3 is the master regulator for the forming of 3D spheroids of 3T3-L1 preadipocytes. *Cells.* 2022; 11: 300.
94. Quan Y, Zhang Y, Li J, Lu F, Cai J. Transplantation of in vitro prefabricated adipose organoids attenuates skin fibrosis by restoring subcutaneous fat and inducing dermal adipogenesis. *FASEB J.* 2023; 37: e23076.
95. Proulx M, Safoine M, Mayrand D, Aubin K, Maux A, Fradette J. Impact of TNF and IL-1 β on capillary networks within engineered human adipose tissues. *J Mater Chem B.* 2016; 4: 3608–19.
96. Proulx M, Mayrand D, Vincent C, Boisvert A, Aubin K, Trottier V, et al. Short-term post-implantation dynamics of *in vitro* engineered human microvascularized adipose tissues. *Biomed Mater.* 2018; 13: 065013.
97. Aubin K, Safoine M, Proulx M, Audet-Casgrain M-A, Côté J-F, Têtu F-A, et al. Characterization of in vitro engineered human adipose tissues: Relevant adipokine secretion and impact of TNF- α . *Karmazyn M, Ed. PLOS ONE.* 2015; 10: e0137612.
98. Oka M, Kobayashi N, Matsumura K, Nishio M, Saeki K. Exogenous cytokine-free differentiation of human pluripotent stem cells into classical brown adipocytes. *Cells.* 2019; 8: 373.
99. Avelino TM, García-Arévalo M, Torres FR, Goncalves Dias MM, Domingues RR, De Carvalho M, et al. Mass spectrometry-based proteomics of 3D cell culture: A useful tool to validate culture of spheroids and organoids. *SLAS Discov.* 2022; 27: 167–74.
100. Daquinag AC, Souza GR, Kolonin MG. Adipose tissue engineering in three-dimensional levitation tissue culture system based on magnetic nanoparticles. *Tissue Eng Part C Methods.* 2013; 19: 336–44.
101. Feng Q, Liu Y, Huang J, Chen K, Huang J, Xiao K. Uptake, distribution, clearance, and toxicity of iron oxide nanoparticles with different sizes and coatings. *Sci Rep.* 2018; 8: 2082.
102. Abakumov MA, Semkina AS, Skorikov AS, Vishnevskiy DA, Ivanova AV, Mironova E, et al. Toxicity of iron oxide nanoparticles: Size and coating effects. *J Biochem Mol Toxicol.* 2018; 32: e22225.
103. Carigil O, Anil-Inevi M, Firatligil-Yildirir B, Unal YC, Yalcin-Ozuyal O, Mese G, et al. Scaffold-free biofabrication of adipocyte structures with magnetic levitation. *Biotechnol Bioeng.* 2021; 118: 1127–40.
104. Slaughter VL, Rumsey JW, Boone R, Malik D, Cai Y, Sriram NN, et al. Validation of an adipose-liver human-on-a-chip model of NAFLD for preclinical therapeutic efficacy evaluation. *Sci Rep.* 2021; 11: 13159.
105. Emont MP, Yu H, Jun H, Hong X, Maganti N, Stegemann JP, et al. Using a 3D culture system to differentiate visceral adipocytes in vitro. *Endocrinology.* 2015; 156: 4761–8.

106. Clevenger TN, Hinman CR, Ashley Rubin RK, Smither K, Burke DJ, Hawker CJ, et al. Vitronectin-based, biomimetic encapsulating hydrogel scaffolds support adipogenesis of adipose stem cells. *Tissue Eng Part A*. 2016; 22: 597–609.
107. Bender R, McCarthy M, Brown T, Bukowska J, Smith S, Abbott RD, et al. Human adipose derived cells in two- and three-dimensional cultures: Functional validation of an *in vitro* fat construct. *Stem Cells Int*. 2020; 2020: 4242130.
108. Yang F, Carmona A, Stojkova K, Garcia Huitron EI, Goddi A, Bhushan A, et al. A 3D human adipose tissue model within a microfluidic device. *Lab Chip*. 2021; 21: 435–46.
109. Mohiuddin OA, Motherwell JM, Rogers E, Bratton MR, Zhang Q, Wang G, et al. Characterization and proteomic analysis of decellularized adipose tissue hydrogels derived from lean and overweight/obese human donors. *Adv Biosyst*. 2020; 4: 2000124.
110. Mohiuddin OA, O'Donnell BT, Poche JN, Iftikhar R, Wise RM, Motherwell JM, et al. Human adipose-derived hydrogel characterization based on *in vitro* ASC biocompatibility and differentiation. *Stem Cells Int*. 2019; 2019: 1–13.
111. Unser AM, Mooney B, Corr DT, Tseng Y-H, Xie Y. 3D brown adipogenesis to create “Brown-fat-in-microstrands”. *Biomaterials*. 2016; 75: 123–34.
112. Lee SY, Park SB, Kim YE, Yoo HM, Hong J, Choi K-J, et al. iTRAQ-based quantitative proteomic comparison of 2D and 3D adipocyte cell models co-cultured with macrophages using online 2D-nanoLC-ESI-MS/MS. *Sci Rep*. 2019; 9: 16746.
113. O'Donnell B, Al-Ghadban S, Ives C, L'Ecuyer M, Monjure T, Romero-Lopez M, et al. Adipose tissue-derived stem cells retain their adipocyte differentiation potential in three-dimensional hydrogels and bioreactors. *Biomolecules*. 2020; 10: 1070.
114. Li X, Xia J, Nicolescu CT, Massidda MW, Ryan TJ, Tien J. Engineering of microscale vascularized fat that responds to perfusion with lipoactive hormones. *Biofabrication*. 2018; 11: 014101.
115. Chen Q, Ruedl C. Obesity retunes turnover kinetics of tissue-resident macrophages in fat. *J Leukoc Biol*. 2020; 107: 773–82.
116. Choi JH, Gimble JM, Vunjak-Novakovic G, Kaplan DL. Effects of hyperinsulinemia on lipolytic function of three-dimensional adipocyte/endothelial co-cultures. *Tissue Eng Part C Methods*. 2010; 16: 1157–65.
117. Lee YS, Olefsky J. Chronic tissue inflammation and metabolic disease. *Genes Dev*. 2021; 35: 307–28.
118. van den Berg SM, van Dam AD, Rensen PCN, de Winther MPJ, Lutgens E. Immune modulation of brown(ing) adipose tissue in obesity. *Endocr Rev*. 2017; 38: 46–68.
119. Taylor J, Sellin J, Kuerschner L, Krähl L, Majlesain Y, Förster I, et al. Generation of immune cell containing adipose organoids for *in vitro* analysis of immune metabolism. *Sci Rep*. 2020; 10: 21104.
120. Anna Ioannidou, Shemim Alatar, Ruby Schipper, Fabiana Baganha, Matilda Åhlander, Amanda Hornell, et al. Hypertrophied human adipocyte spheroids as *in vitro* model of weight gain and adipose tissue dysfunction. *J Physiol*. 2022; 600: 869–83.
121. Rajangam T, Park MH, Kim S-H. 3D human adipose-derived stem cell clusters as a model for *in vitro* fibrosis. *Tissue Eng Part C Methods*. 2016; 22: 679–90.
122. Choi KJ, Lee JH, Park SB, Na Y-J, Jung WH, Lee H, et al. Development of *in vitro* three-dimensional drug screening system for obesity-related metabolic syndrome. *J Pharmacol Sci*. 2022; 148: 377–86.
123. Tharp KM, Jha AK, Kraiczky J, Yesian A, Karateev G, Sinisi R, et al. Matrix-assisted transplantation of functional beige adipose tissue. *Diabetes*. 2015; 64(11): 3713–24.
124. Aiming for equitable precision medicine in diabetes. *Nat Med*. 2022; 28: 2223.
125. Zimmet P, Shi Z, El-Osta A, Ji L. Epidemic T2DM, early development and epigenetics: Implications of the Chinese famine. *Nat Rev Endocrinol*. 2018; 14: 738–46.
126. Van Nguyen T-T, Van Vu V, Van Pham P. Transcriptional factors of thermogenic adipocyte development and generation of brown and beige adipocytes from stem cells. *Stem Cell Rev Rep*. 2020; 16: 876–92.
127. Johnson AMF, Olefsky JM. The origins and drivers of insulin resistance. *Cell*. 2013; 152: 673–84.
128. Klein S, Gastaldelli A, Yki-Järvinen H, Scherer PE. Why does obesity cause diabetes? *Cell Metab*. 2022; 34: 11–20.
129. Magkos F, Hjorth MF, Astrup A. Diet and exercise in the prevention and treatment of type 2 diabetes mellitus. *Nat Rev Endocrinol*. 2020; 16: 545–55.
130. American Diabetes Association Professional Practice Committee. 3. Prevention or delay of type 2 diabetes and associated comorbidities: Standards of medical care in diabetes—2022. *Diabetes Care*. 2021; 45: S39–45.
131. Chellappan DK, Yap WS, Bt Ahmad Suhaimi NA, Gupta G, Dua K. Current therapies and targets for type 2 diabetes mellitus. *Paininerva Med*. 2018; 60: 117–31.
132. White JD, Dewal RS, Stanford KI. The beneficial effects of brown adipose tissue transplantation. *Mol Aspects Med*. 2019; 68: 74–81.
133. Pirillo A, Casula M, Olmastroni E, Norata GD, Catapano AL. Global epidemiology of dyslipidaemias. *Nat Rev Cardiol*. 2021; 18: 689–700.
134. Younossi ZM, Golabi P, de Avila L, Paik JM, Srishord M, Fukui N, et al. The global epidemiology of NAFLD and NASH in patients with type 2 diabetes: A systematic review and meta-analysis. *J Hepatol*. 2019; 71: 793–801.
135. Polyzos SA, Kountouras J, Mantzoros CS. Obesity and nonalcoholic fatty liver disease: From pathophysiology to therapeutics. *Metabolism*. 2019; 92: 82–97.
136. Powell EE, Wong VW-S, Rinella M. Non-alcoholic fatty liver disease. *Lancet Lond Engl*. 2021; 397: 2212–24.
137. Katsiki N, Mikhailidis DP, Mantzoros CS. Non-alcoholic fatty liver disease and dyslipidemia: An update. *Metabolism*. 2016; 65: 1109–23.
138. Vekic J, Zeljkovic A, Stefanovic A, Jelic-Ivanovic Z, Spasojevic-Kalimanovska V. Obesity and dyslipidemia. *Metabolism*. 2019; 92: 71–81.
139. Berberich AJ, Hegele RA. A modern approach to dyslipidemia. *Endocr Rev*. 2022; 43: 611–53.
140. Low LA, Mummery C, Berridge BR, Austin CP, Tagle DA. Organs-on-chips: into the next decade. *Nat Rev Drug Discov*. 2021; 20: 345–61.
141. Singh AM, Dalton S. What can ‘brown-ing’ do for you? *Trends Endocrinol Metab*. 2018; 29: 349–59.
142. Chal J, Oginuma M, Al Tanoury Z, Gobert B, Sumara O, Hick A, et al. Differentiation of pluripotent stem cells to muscle fiber to model Duchenne muscular dystrophy. *Nat Biotechnol*. 2015; 33: 962–9.
143. Han X, Wang M, Duan S, Franco PJ, Kenty JH-R, Hedrick P, et al. Generation of hypoinmunogenic human pluripotent stem cells. *Proc Natl Acad Sci U S A*. 2019; 116: 10441–6.
144. Hafner AL, Mohsen-Kanson T, Dani C. Differentiation of brown adipocyte progenitors derived from human induced pluripotent stem cells. *Methods Mol Biol*. 2018; 1773: 31–39.
145. Palani NP, Horvath C, Timshele PN, Folkertsma P, Grønning AGB, Henriksen TI, et al. Adipogenic and SWAT cells separate from a common progenitor in human brown and white adipose depots. *Nat Metab*. 2023; 5: 996–1013.
146. Di Franco A, Guasti D, Squecco R, Mazzanti B, Rossi F, Idrizaj E, et al. Searching for classical brown fat in humans: Development of a novel human fetal brown stem cell model. *Stem Cells*. 2016; 34: 1679–91.
147. Nishikawa S, Aoyama H, Kamiya M, Higuchi J, Kato A, Soga M, et al. Artepillin C, a typical brazilian propolis-derived component, induces brown-like adipocyte formation in C3H10T1/2 cells, primary inguinal white adipose tissue-derived adipocytes, and mice. *PLoS ONE*. 2016; 11: e0162512.
148. Wang X, Chen J, Rong C, Pan F, Zhao X, Hu Y. GLP-1RA promotes brown adipogenesis of C3H10T1/2 mesenchymal stem cells via the PI3K-AKT-mTOR signaling pathway. *Biochem Biophys Res Commun*. 2018; 506: 976–82.
149. Cave E, Crowther NJ. The use of 3T3-L1 murine preadipocytes as a model of adipogenesis. *Methods Mol Biol*. 2019; 1916: 263–272.
150. Takeda Y, Dai P. A developed serum-free medium and an optimized chemical cocktail for direct conversion of human dermal fibroblasts into brown adipocytes. *Sci Rep*. 2020; 10: 3775.
151. Takeda Y, Harada Y, Yoshikawa T, Dai P. Direct conversion of human fibroblasts to brown adipocytes by small chemical compounds. *Sci Rep*. 2017; 7: 4304.
152. Guan Q, Wang Z, Cao J, Dong Y, Chen Y. Mechanisms of melatonin in obesity: A review. *Int J Mol Sci*. 2021; 23: 218.
153. Van Den Berg R, Kooijman S, Noordam R, Ramkisoensing A, Abreu-Vieira G, Tambyrajah LL, et al. A diurnal rhythm in brown adipose tissue causes rapid clearance and combustion of plasma lipids at waking. *Cell Rep*. 2018; 22: 3521–33.
154. Alvarez-Dominguez JR, Donaghey J, Rasouli N, Kenty JHR, Helman A, Charlton J, et al. Circadian entrainment triggers maturation of human *in vitro* islets. *Cell Stem Cell*. 2020; 26: 108–122.e10.
155. Massier L, Jalkanen J, Elmastas M, Zhong J, Wang T, Nono Nankam PA, et al. An integrated single cell and spatial transcriptomic map of human white adipose tissue. *Nat Commun*. 2023; 14: 1438.
156. Emont MP, Jacobs C, Essene AL, Pant D, Tenen D, Colleluori G, et al. A single-cell atlas of human and mouse white adipose tissue. *Nature*. 2022; 603: 926–33.
157. Lenz M, Arts ICW, Peeters RLM, de Kok TM, Ertaylan G. Adipose tissue in health and disease through the lens of its building blocks. *Sci Rep*. 2020; 10: 10433.

158. Lee HJ, Lee J, Yang MJ, Kim Y-C, Hong SP, Kim JM, et al. Endothelial cell-derived stem cell factor promotes lipid accumulation through c-Kit-mediated increase of lipogenic enzymes in brown adipocytes. *Nat Commun.* 2023; 14: 2754.
159. Ichida JK, Ko CP. Organoids develop motor skills: 3D human neuromuscular junctions. *Cell Stem Cell.* 2020 Feb 6;26(2):131-133.
160. Faustino Martins J-M, Fischer C, Urzi A, Vidal R, Kunz S, Ruffault P-L, et al. Self-organizing 3D human trunk neuromuscular organoids. *Cell Stem Cell.* 2020; 26: 172-186.e6.
161. Pellegriinelli V, Rouault C, Veyrie N, Clément K, Lacasa D. Endothelial cells from visceral adipose tissue disrupt adipocyte functions in a three-dimensional setting: Partial rescue by angiotensin-1. *Diabetes.* 2014; 63: 535-49.
162. Buckberry S, Liu X, Poppe D, Tan JP, Sun G, Chen J, et al. Transient naive reprogramming corrects hiPS cells functionally and epigenetically. *Nature.* 2023; 620: 863-72.
163. Pepper AR, Gala-Lopez B, Pawlick R, Merani S, Kin T, Shapiro AMJ. A prevascularized subcutaneous device-less site for islet and cellular transplantation. *Nat Biotechnol.* 2015; 33: 518-23.
164. Yoshihara E, O'Connor C, Gasser E, Wei Z, Oh TG, Tseng TW, et al. Immune-evasive human islet-like organoids ameliorate diabetes. *Nature.* 2020; 586: 606-11.
165. Ding S, Hsu C, Wang Z, Natesh NR, Millen R, Negrete M, et al. Patient-derived micro-organospheres enable clinical precision oncology. *Cell Stem Cell.* 2022; 29: 905-917.e6.
166. Zhou X, Li Z, Qi M, Zhao P, Duan Y, Yang G, et al. Brown adipose tissue-derived exosomes mitigate the metabolic syndrome in high fat diet mice. *Theranostics.* 2020; 10: 8197-210.
167. Scheele C, Wolfrum C. Brown adipose crosstalk in tissue plasticity and human metabolism. *Endocr Rev.* 2020; 41: 53-65.
168. Niemann B, Haufs-Brusberg S, Puetz L, Feickert M, Jaekstein MY, Hoffmann A, et al. Apoptotic brown adipocytes enhance energy expenditure via extracellular inosine. *Nature.* 2022; 609: 361-8.
169. Rosina M, Ceci V, Turchi R, Chuan L, Borcharding N, Sciarretta F, et al. Ejection of damaged mitochondria and their removal by macrophages ensure efficient thermogenesis in brown adipose tissue. *Cell Metab.* 2022; 34: 533-548.e12.
170. Becher T, Palanisamy S, Kramer DJ, Eljalby M, Marx SJ, Wibmer AG, et al. Brown adipose tissue is associated with cardiometabolic health. *Nat Med.* 2021; 27: 58-65.